Atmospheric Tomography
The Odin/OSIRIS Experience

E.J. Llewellyn, D.A. Degenstein, N.D. Lloyd, R.L. Gattinger
ISAS, University of Saskatchewan
Saskatoon, SK, S7N 5E2
Canada
and
I.C. McDade
EATS, York University
Toronto, ON, M3J 1P3
Canada
edward.llewellyn@usask.ca

The Four Musketeers

Dr. Nick Lloyd *Dr. Doug Degenstein* *Dr. Ian McDade* *Dr. Dick Gattinger*

This group have made OSIRIS tomography a reality.

Outline

- What is tomography?
- Line integrals
- Inversion of a line integral, the adopted approach.
- How did we get into it? Stan Solomon did it with AE.
- Reverse digital filtering, frequencies are added not removed.
- Non-stationary simulations.
- Requirement for an imager, you can construct an image.
- Examples from OSIRIS.
- Looking out of plane.
- Improving the horizontal resolution.

Tomography (from the Greek *tomos*, to slice) is the representation of a three dimensional object by means of its two dimensional cross sections.

For most tomographic applications this requires the solution of a system of equations that consist of many line integrals that are represented in a discrete fashion.

Such techniques have been extensively applied in the field of medical imaging but are still in their infancy for atmospheric investigations.

The Geometry To Scale for Limb Observations

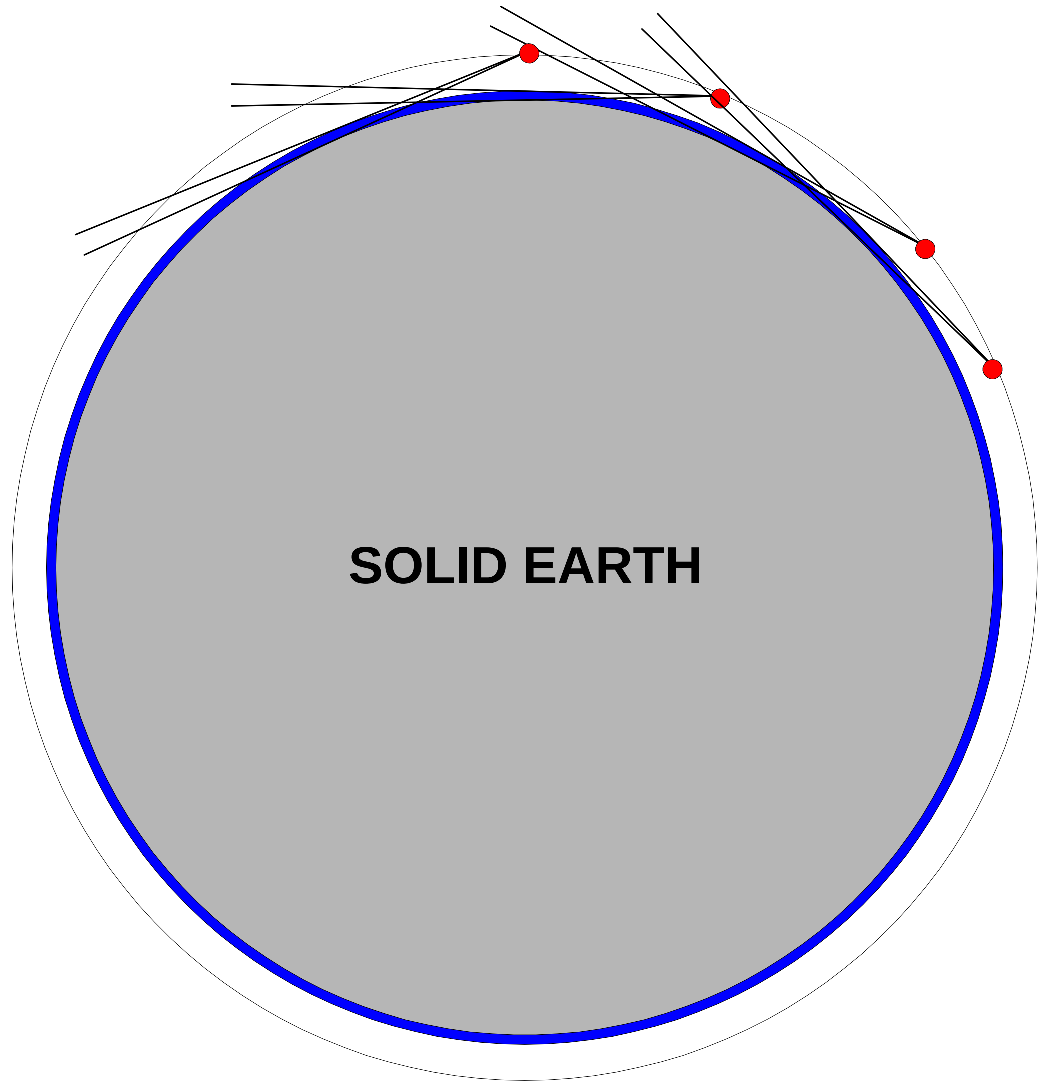

Satellite Orbit : 6978 km
Satellite Speed : 7.559 km/s
Satellite Period : 96.7 min

The blue annulus is the atmosphere below 100 km.

A Single Observation

Observations : $\boldsymbol{O_i}$
Volume Emission Elements : $\boldsymbol{V_j}$

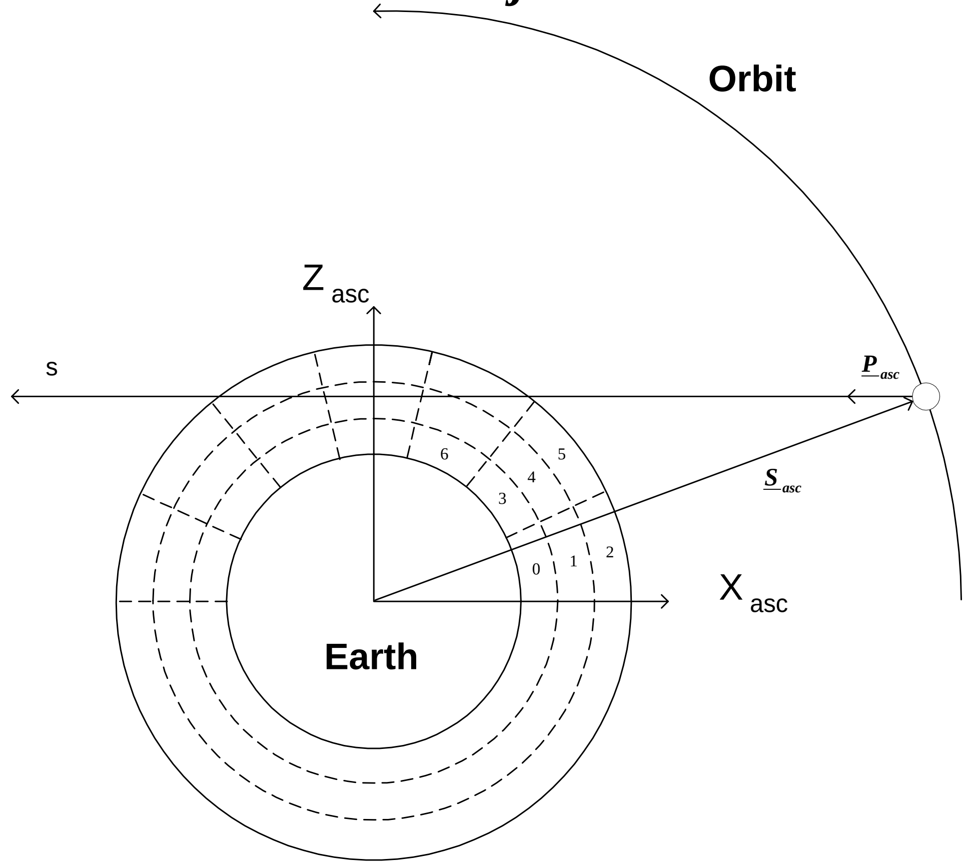

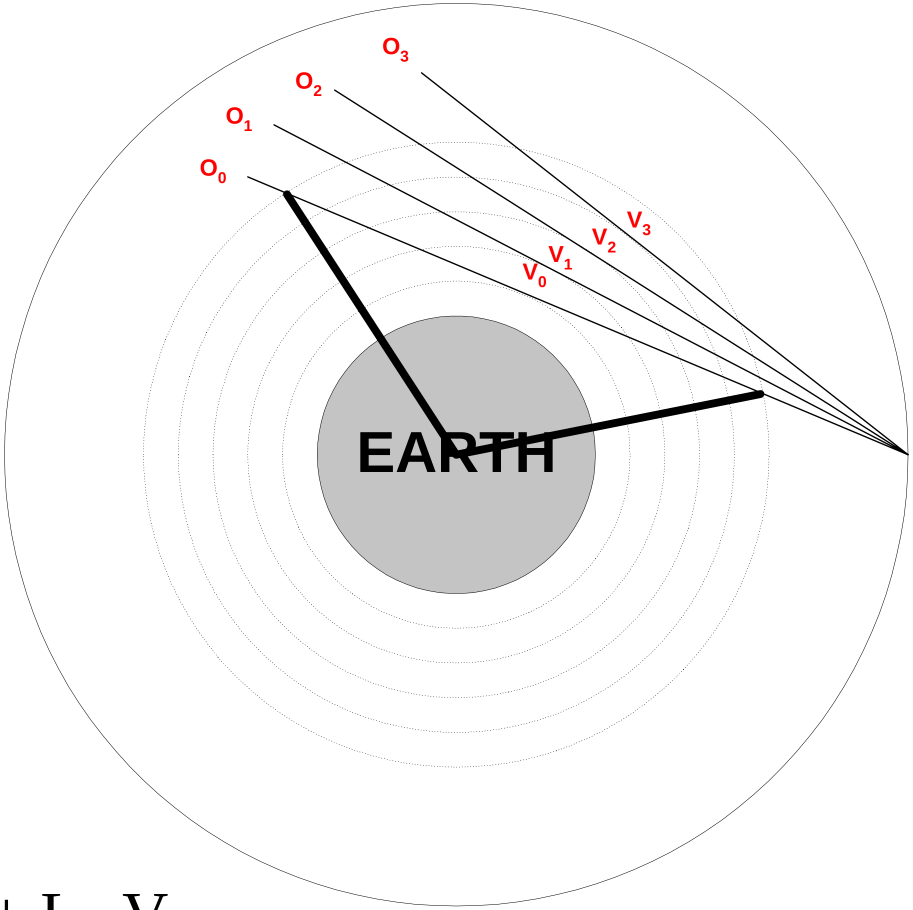

A Simple Geometry

$$
\begin{aligned}
O_0 &= L_{00}V_{00} + L_{01}V_1 + L_{02}V_2 + L_{03}V_3 \\
O_1 &= L_{11}V_1 + L_{12}V_2 + L_{13}V_3 \\
O_2 &= L_{22}V_2 + L_{23}V_3 \\
O_3 &= L_{33}V_3
\end{aligned}
$$

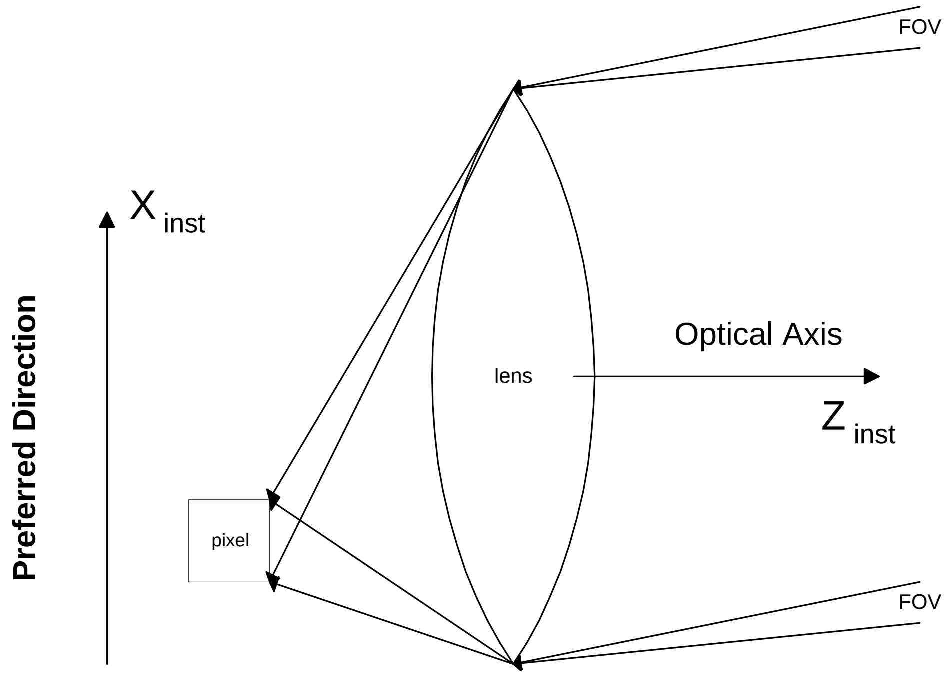

Simple imager instrument representation; the indicated FOV is that for a single pixel.

The observed brightness is the integral of the volume emission contributions along the line of sight.

$$O_{\underline{p}_{asc}} = \int_{sat}^{\infty} V(s)\,ds$$

This integral can be discretely represented as

$$O_{\underline{p}_{asc}} = \sum_{j} L_{\underline{p}_{asc},j} V_j \quad [kR]$$

Where $L_{\underline{p}_{asc},j}$ $[km]$ geometric path is the length through each element and V_j $\left[{kR}/{km}\right]$ is the volume emission contribution from each element j

The Line of Sight (black line) along a structured Limb Emission

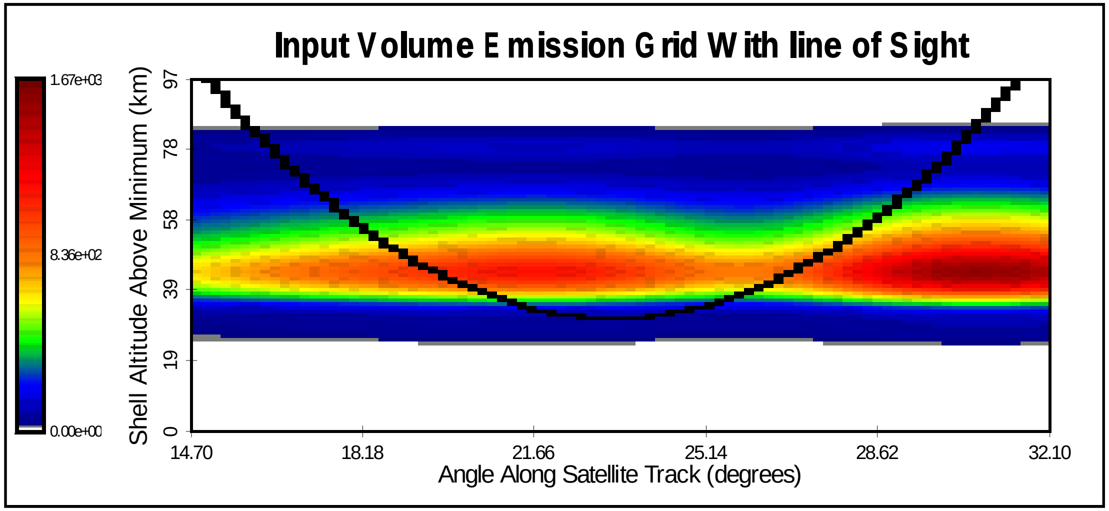

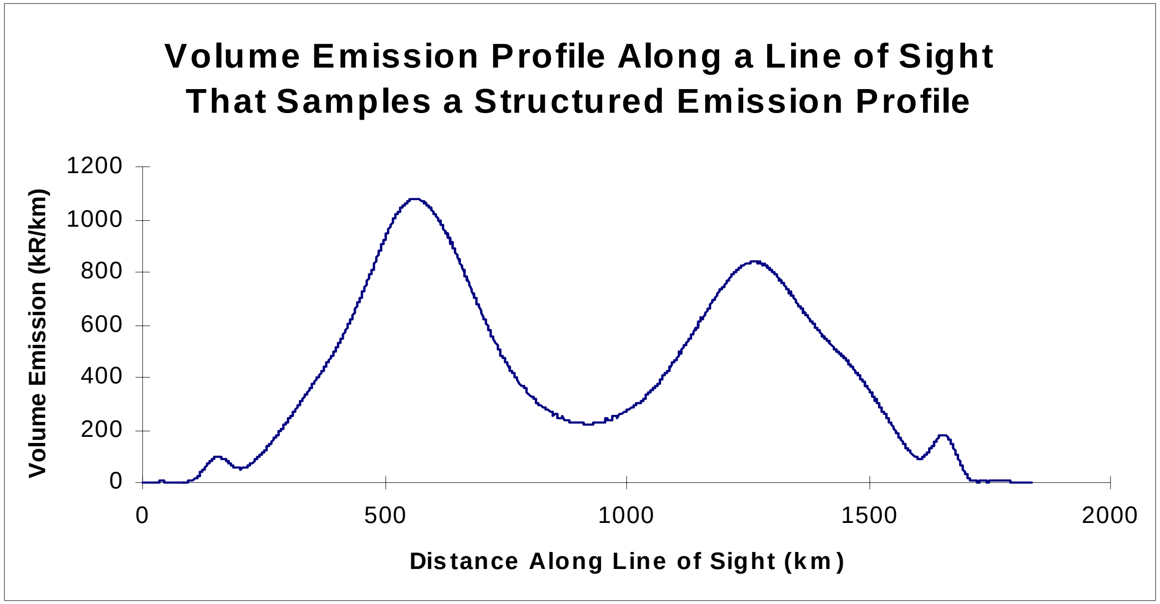

Retrieval of a structured emission from a series of Limb images that are inverted individually with the assumption of horizontal homogeneity.

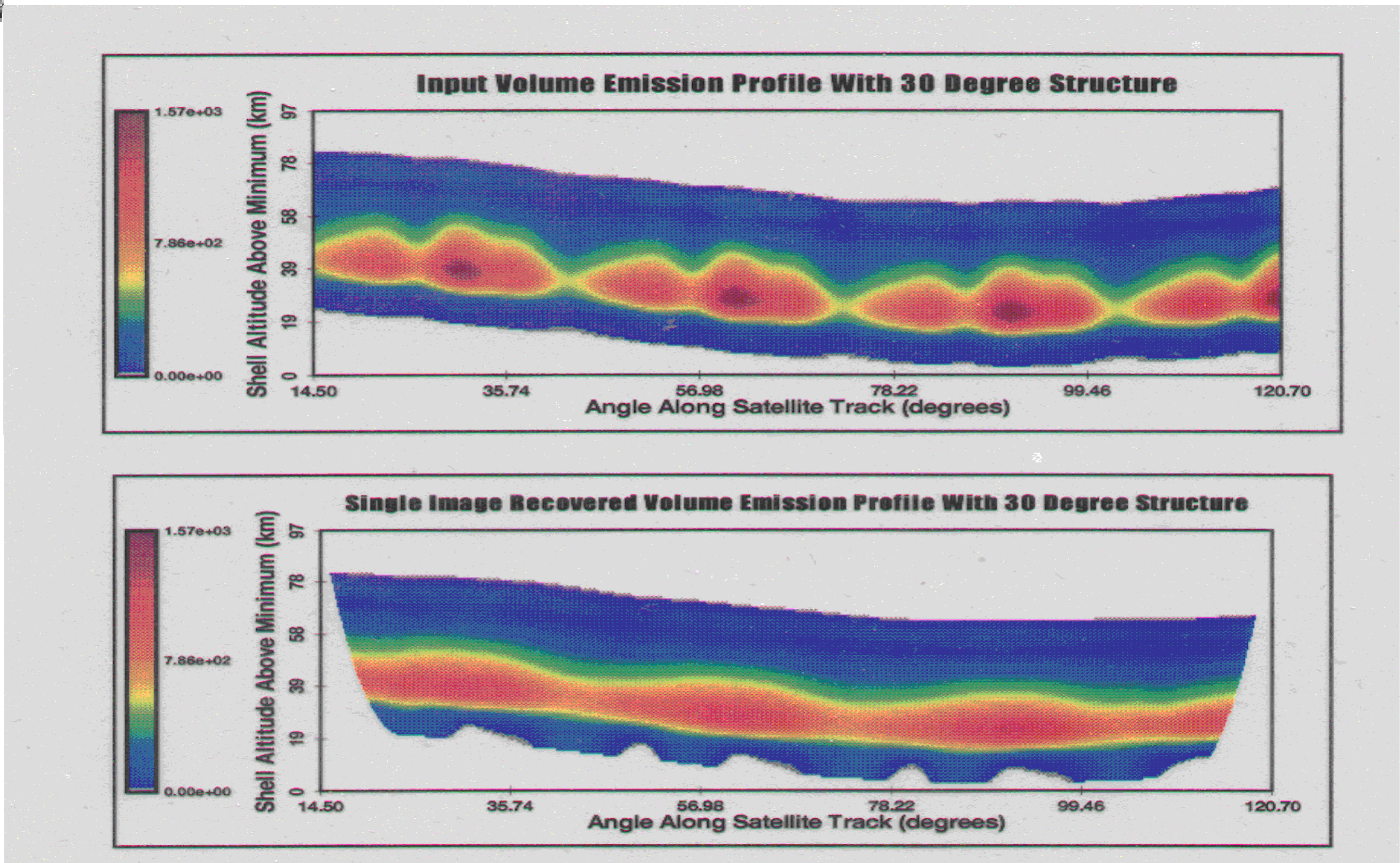

The previous slide shows that the volume emission contributions along the line of sight are not well recovered.

$$O_{\underline{p}_{asc}} = \int_{sat}^{\infty} V(s)\,ds$$

The retrieved V(s) values are some form of average. Obviously for observations across the terminator the solar conditions are not constant and the value of any inversion is limited. A real terminator satellite is Odin.

Thus for an accurate retrieval of the structure the assumption of homogeneity must be eliminated.

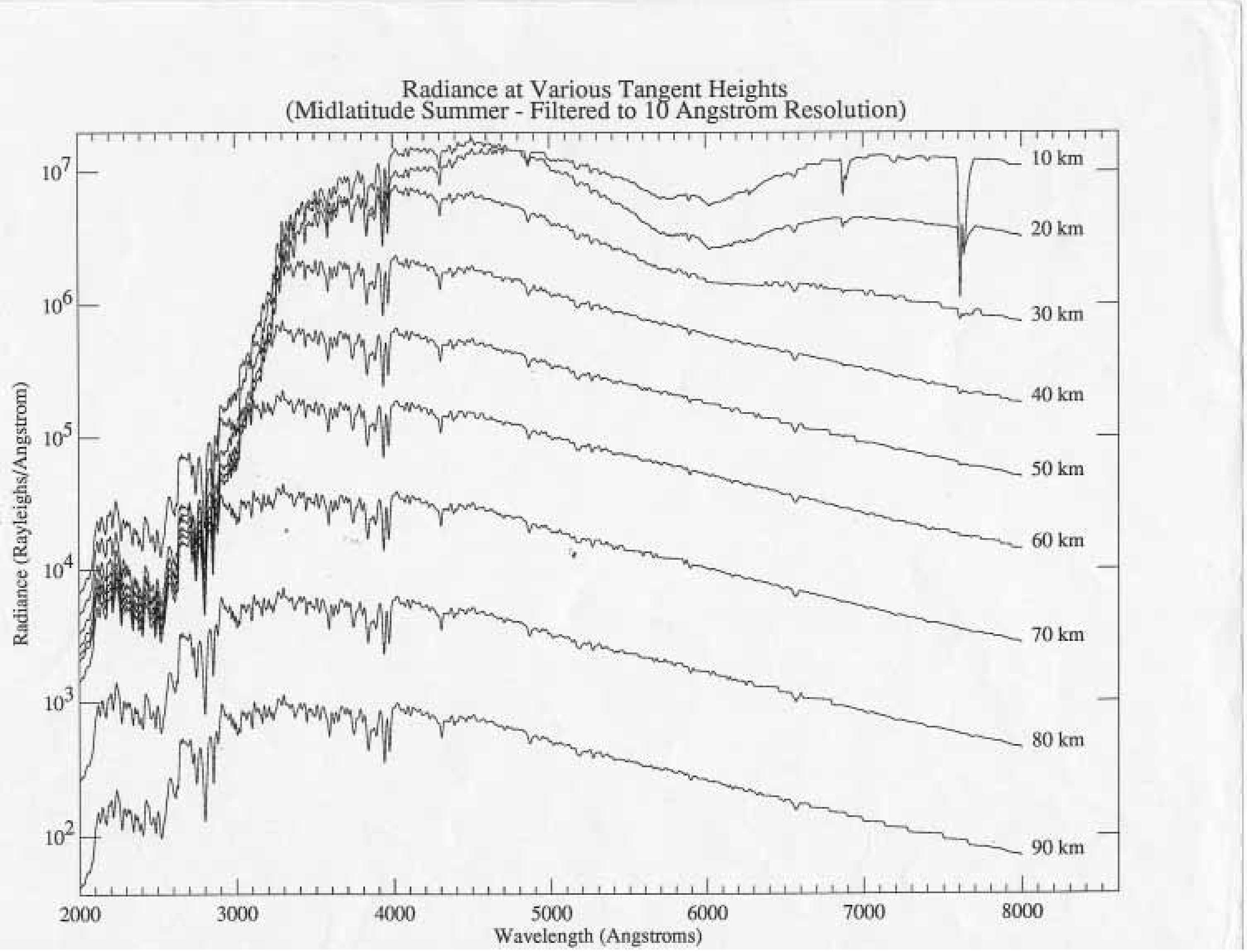

The figure shows the required dynamic range for a limb viewing imager

The practical realization of Satellite Tomography-1

Any instrument must have a wide dynamic range, ~10^7 for observations in the visible region in the limb.

Any instrument must have minimum spectral cross-talk, ~10^{-6} for 1 nm resolution in the visible region.

Any instrument must have good baffle rejection, *i.e.* baffle scattering must be minimized.

Instrument response time must be appropriate for the imaging rate.

Pixel blurring must be minimal.

The practical realization of Satellite Tomography-2

The Odin satellite has two instruments that both observe the atmospheric limb in the orbit plane.

A sub-millimetre/millimetre radiometer (SMR)

An optical spectrograph infrared imager system (OSIRIS)

The OS slit (1km x 40km) is oriented parallel to the limb.

The IRI detector (110km x 2km) is oriented perpendicular to the limb. The vertical FOV of each pixel is 1 km.

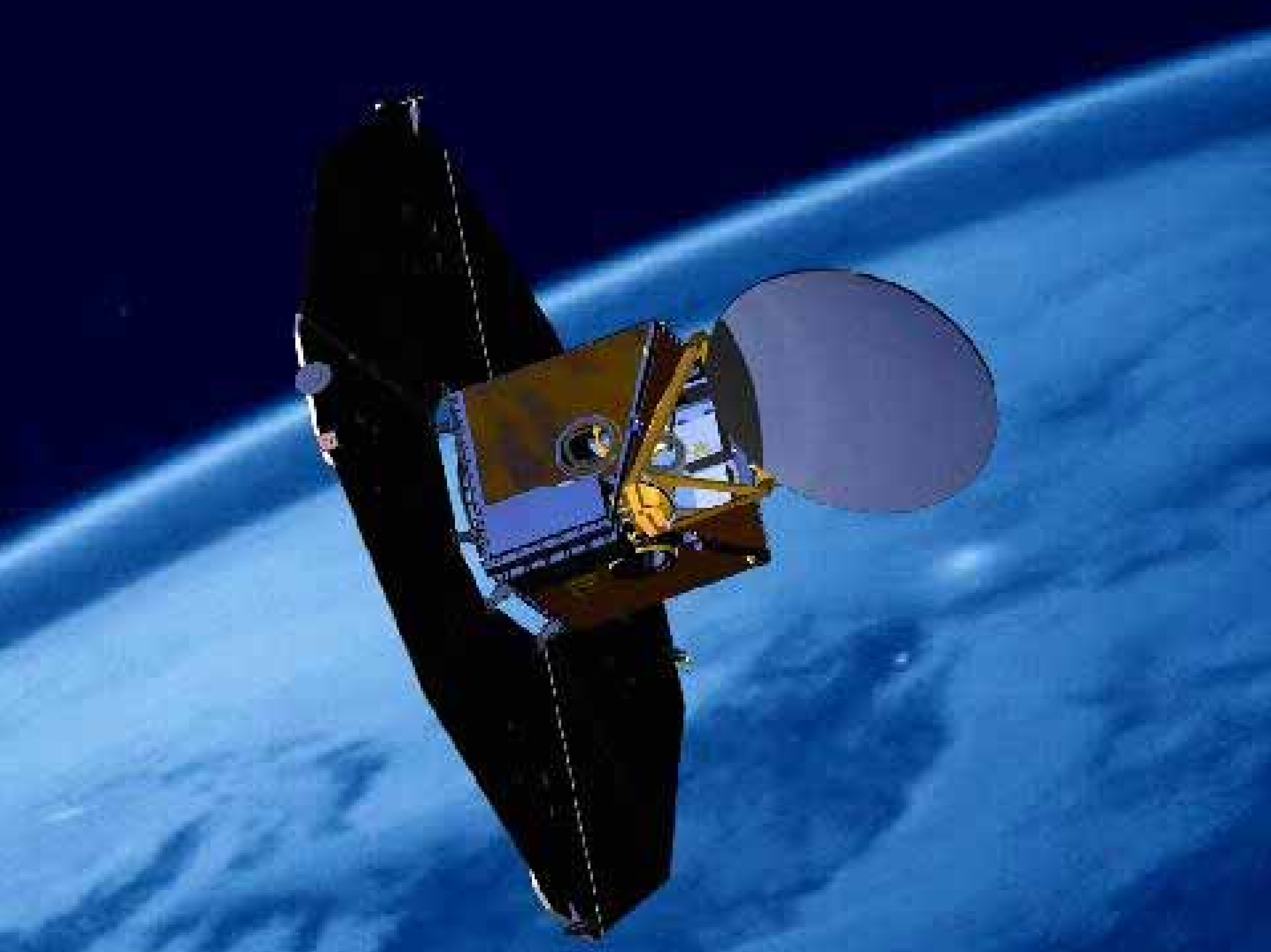

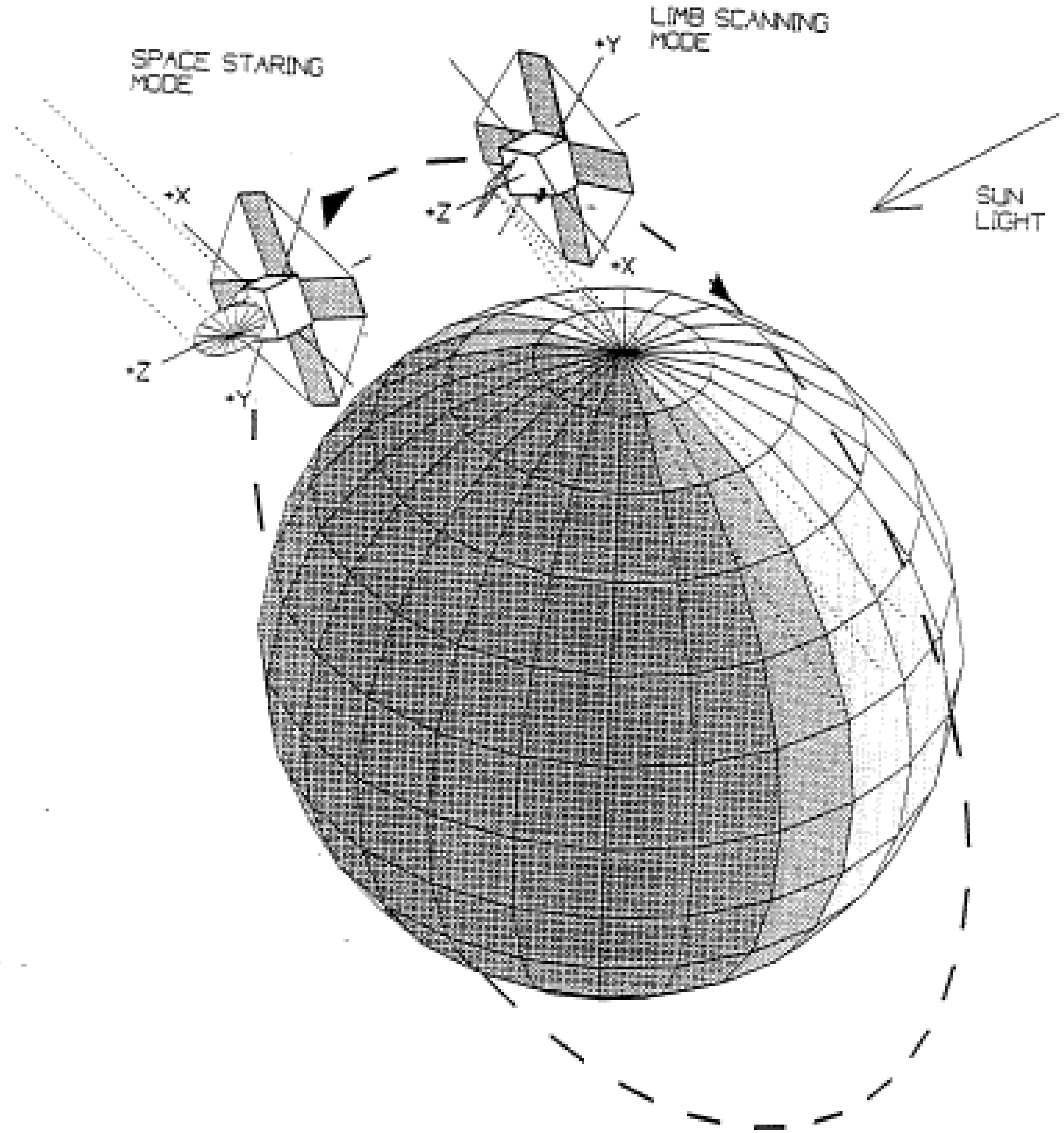

The Odin orbit is sun-synchronous with the ascending node at 1800LT

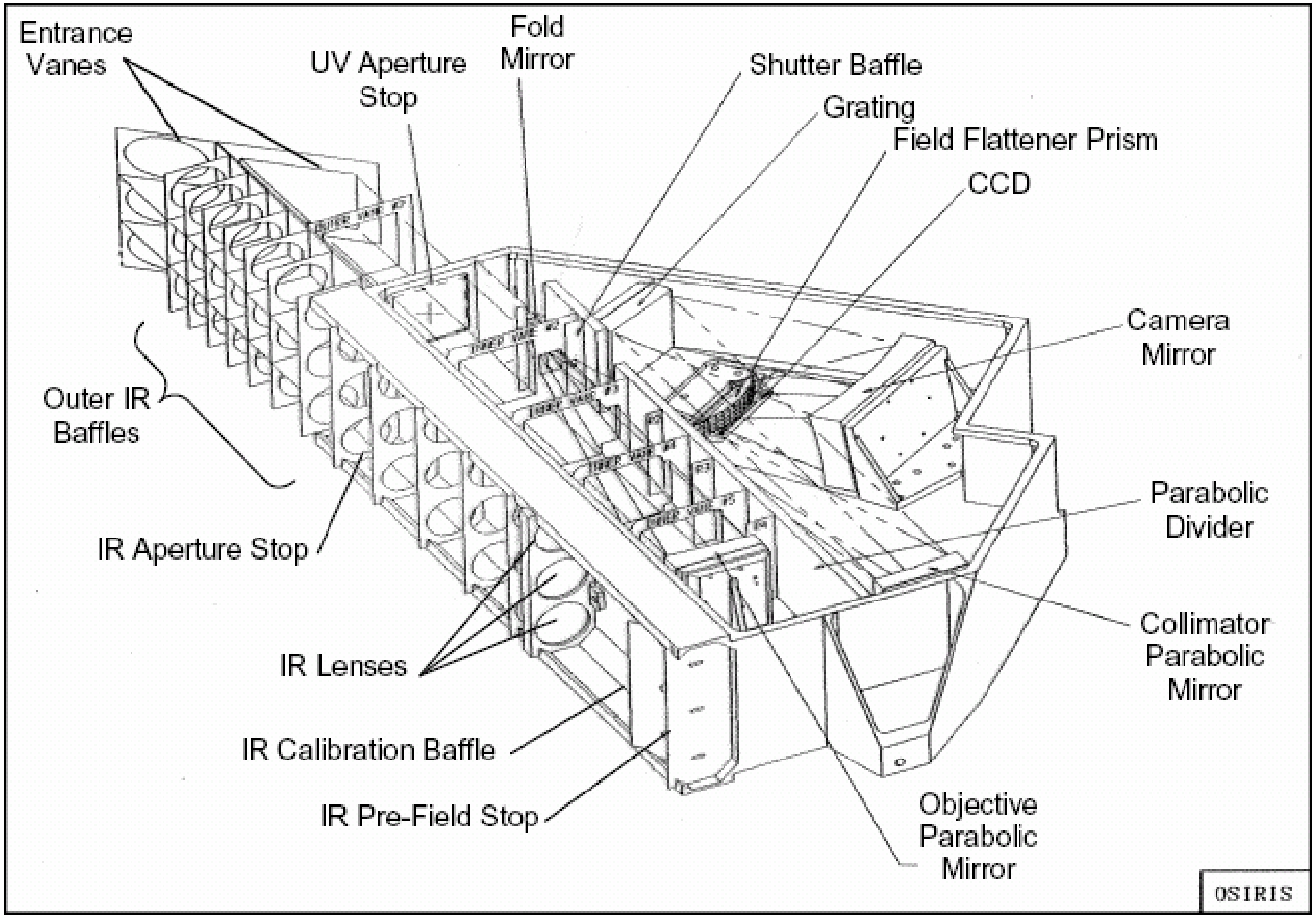

Wireframe diagram of OSIRIS (Wiensz, 2005)

OSIRIS on the bench at the Svobodny Cosmodrome, Siberia

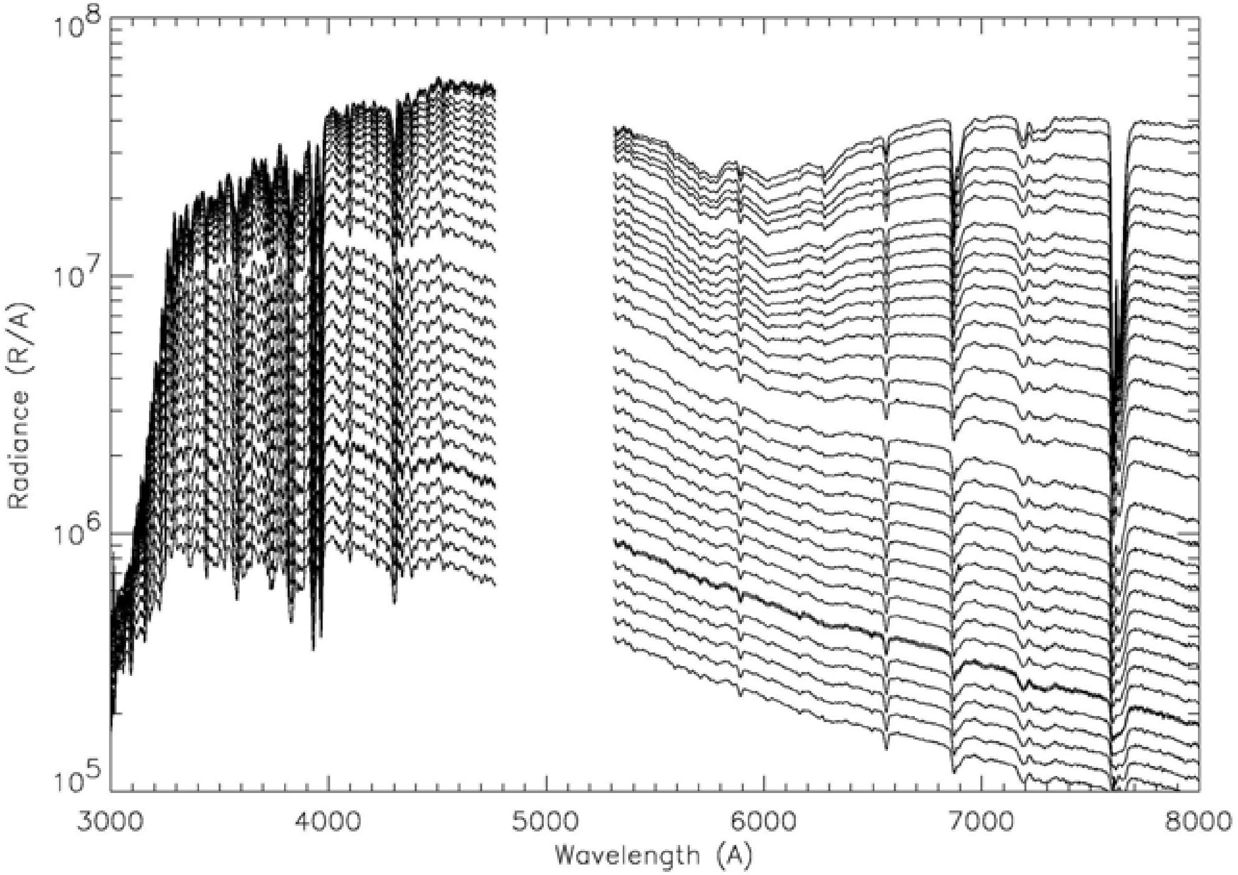

Optical spectrograph Limb Scan from 10 – 60 km.
Location ~80 N, 0 W.
Missing region is at the position of the order sorter.

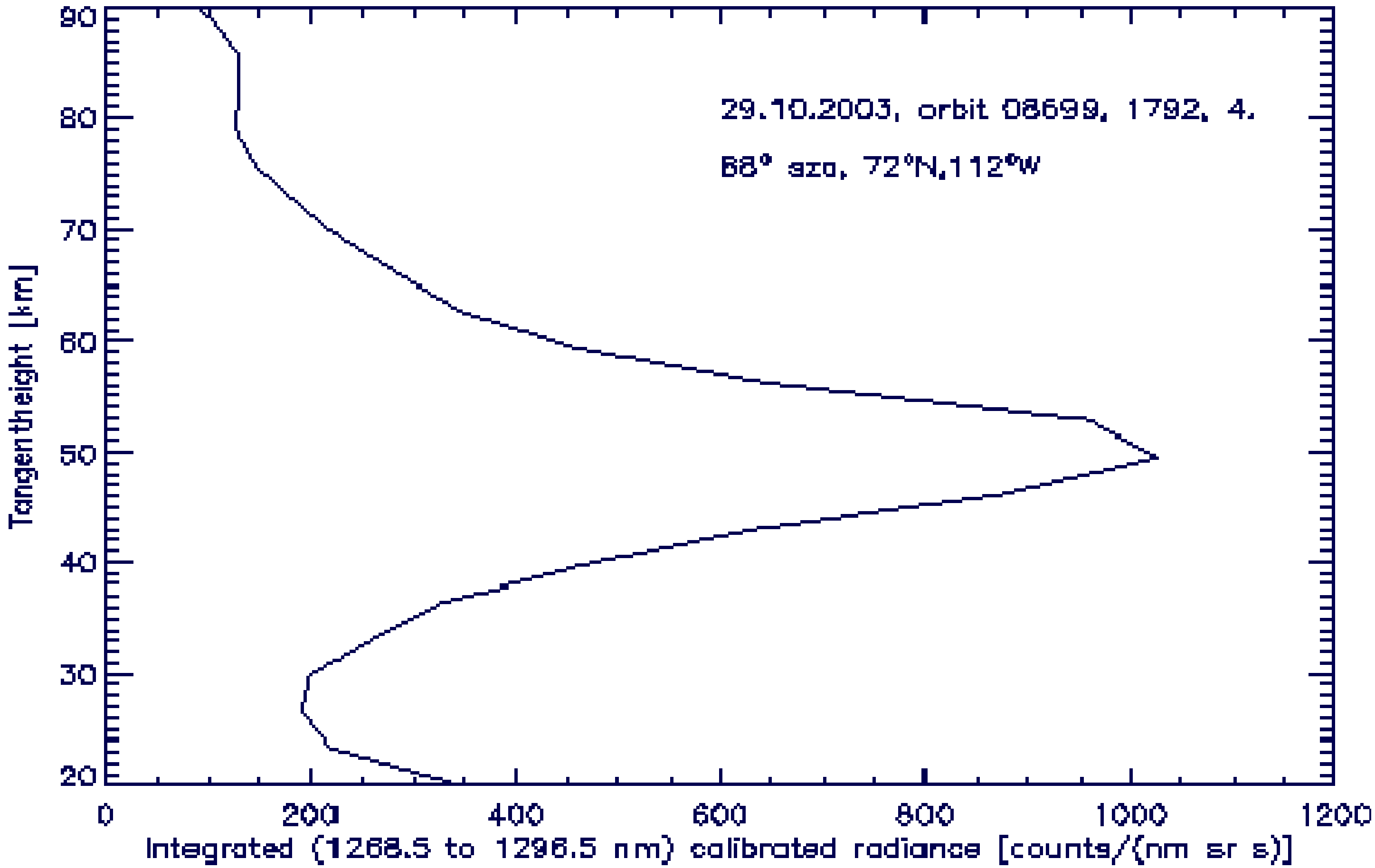

OSIRIS Infrared Imager Limb Image of the OIRA dayglow.

The Geometry To Scale for Limb Observations

Satellite Orbit : 6978 km
Satellite Speed : 7.559 km/s
Satellite Period : 96.7 min

The blue annulus is the atmosphere below 100 km.

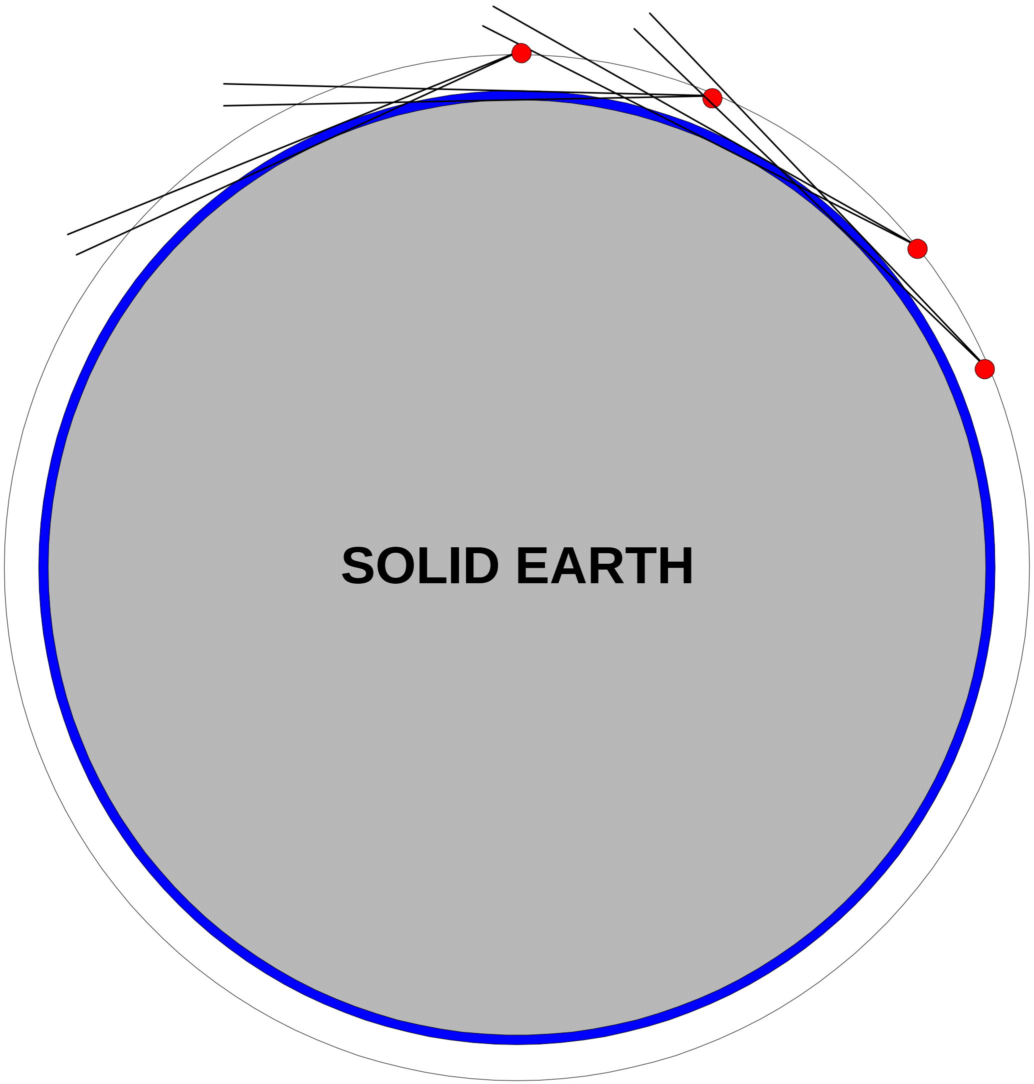

Limb Imaging from Space

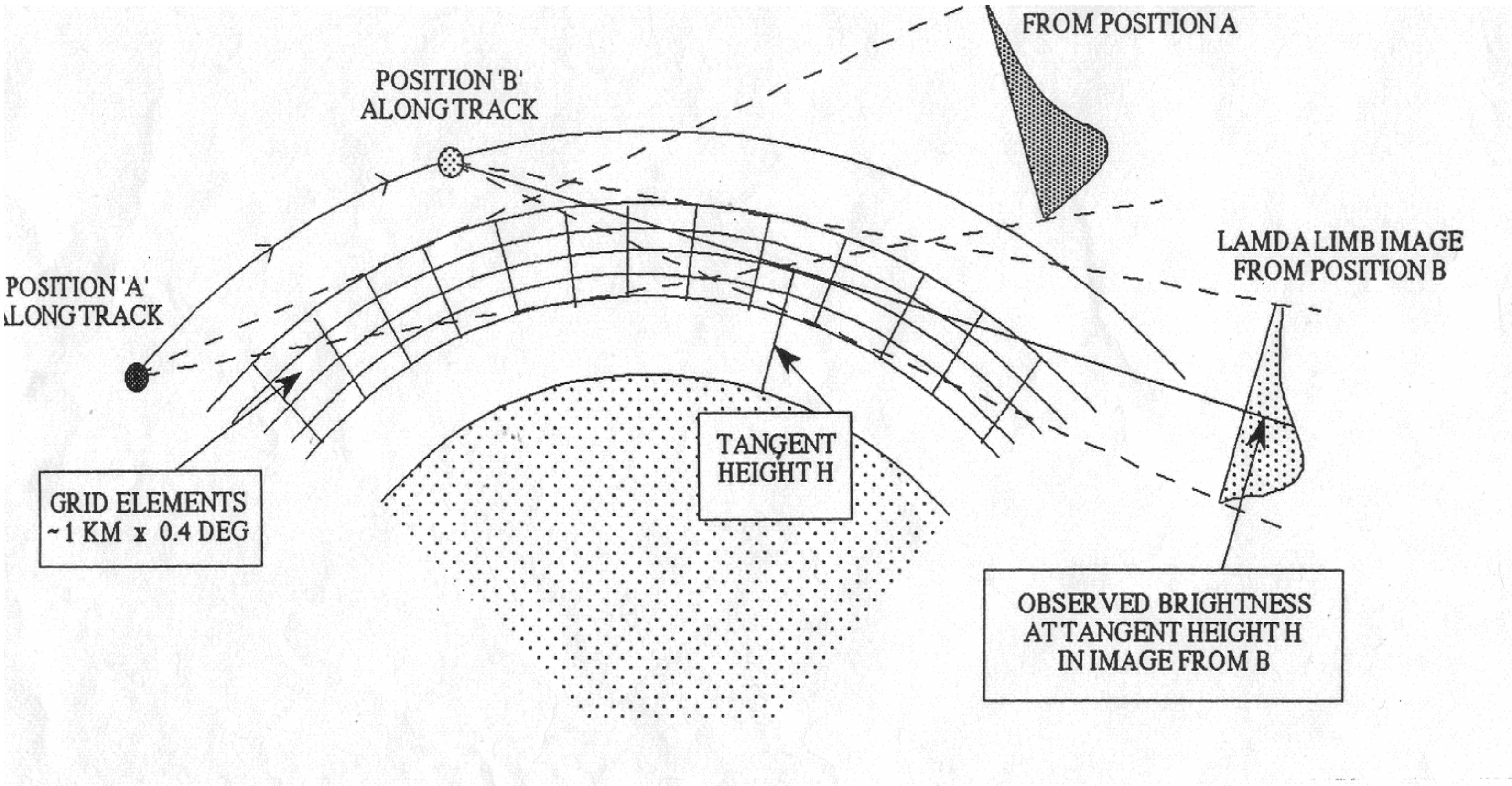

The basic matrix equation that has to be solved is

$$\boldsymbol{B} = \boldsymbol{AT}$$

where

B is the measured image,

A is an apparatus dependent parameter,

T is the contribution of each element to the image, Initial approach used to deblur Fabry-Perot images that were compressed with the assumption of circular rings.

Maximum Probability (MP) method - the most probable contribution of any element j to the measurement B_i, given that the T_j values are distributed according to photon counting, or Poisson, statistics. The concept is that each T_j value is the mean value, given that the contribution of that object element to the image is P_{ij}, and in the mean $P_{ij} = A_{ij}T_j$.

The actual equations used were:

$$P_{ij} = \frac{\left(B_i + n_i\right) A_{ij} T_j}{\sum_j A_{ij} T_j} - 1$$

$$T_j = \frac{\sum_i P_{ij}}{\sum_i A_{ij}}$$

where P_{ij} is the most probable value of the contribution to the measurement B_i, given that the mean value of the object is T_j and n_i is the number of elements that contribute to measurement i. These equations are iterative.

The Tomographic Equations

Original Lloyd, McDade and Llewellyn equations

$$P_{ij} = \frac{(O_i + n_i)L_{ij}V_j}{\sum_j L_{ij}V_j} - 1$$

$$V_j = \frac{\sum_i P_{ij}}{\sum_i L_{ij}}$$

Modified Equations

$$V_j^{(n)} = V_j^{(n-1)} \sum_i \left(\frac{O_i}{O_{i_{est}}^{(n-1)}} \beta_{ij} \right)$$

where

$$\sum_j L_{ij} V_j^{(n-1)} = O_{i_{est}}^{(n-1)}$$

and

$$\frac{L_{ij}^m}{\sum_i L_{ij}^m} = \beta_{ij}$$

with

$$\sum_i \beta_{ij} = 1$$

OSIRIS Tomography

The Tomographic Algorithm

$$V_j^{(n)} = V_j^{(n-1)} \sum_i \left(\frac{O_i}{O_{i_{est}}^{(n-1)}} \beta_{ij} \right)$$

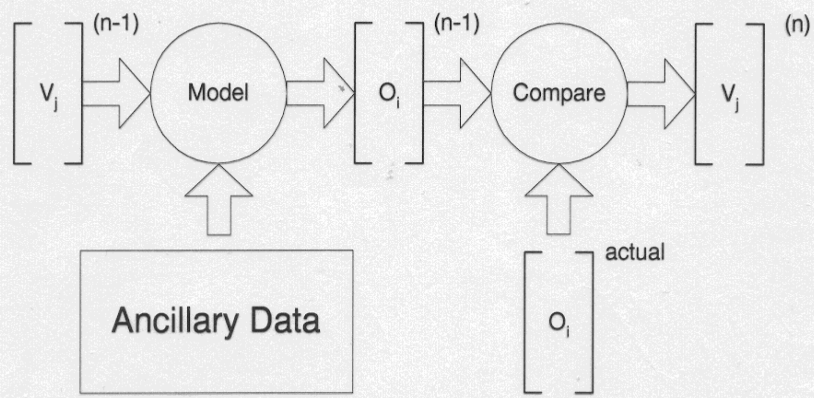

Note : For 700 images taken once every two seconds and a grid cell size of 1 km by 0.2° there are 70,000 observations and 54,000 grid cells.

The initial estimate is $V_j^{(1)} = \sum_i \left(\frac{O_i}{\sum_j L_{ij}} \beta_{ij} \right)$

The termination condition is a fixed number of iterations.

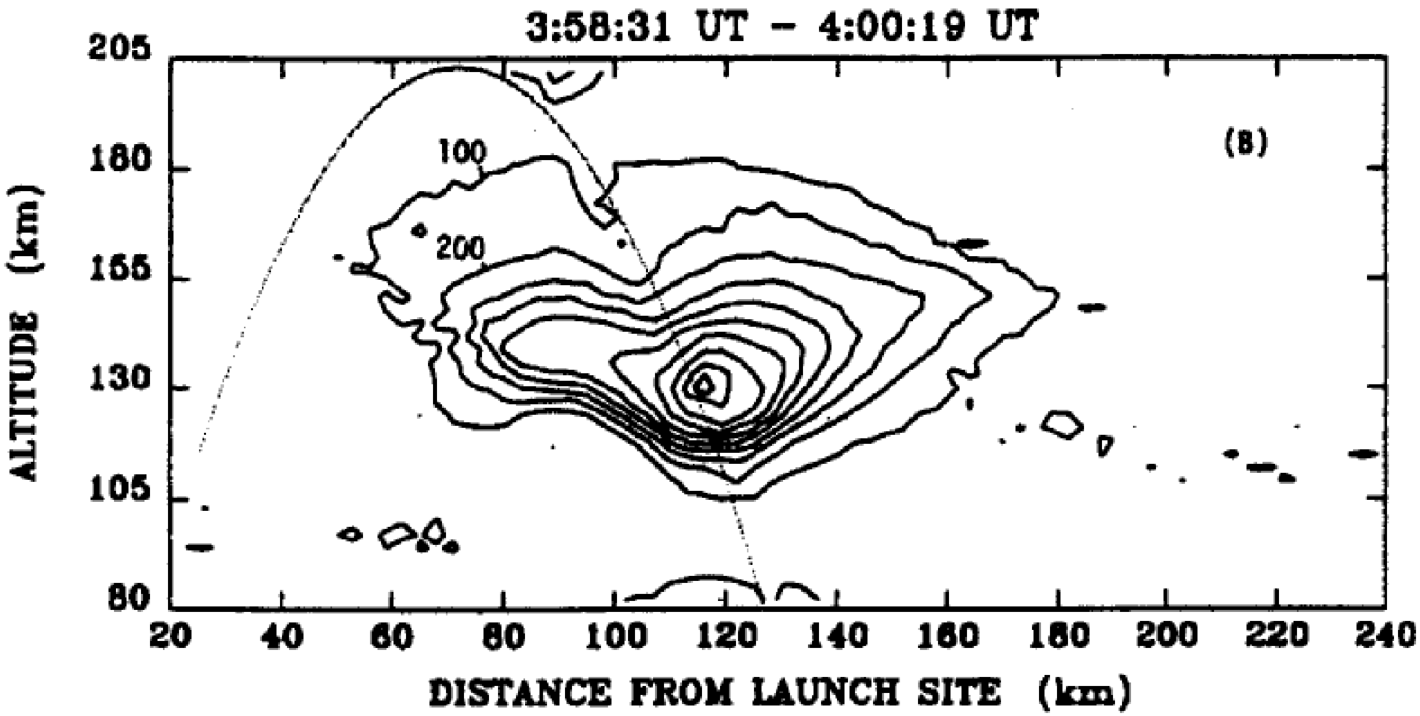

Tomographic retrieval of the auroral distribution seen on ARIES – after McDade et al.

Model runs of the OSIRIS Tomography

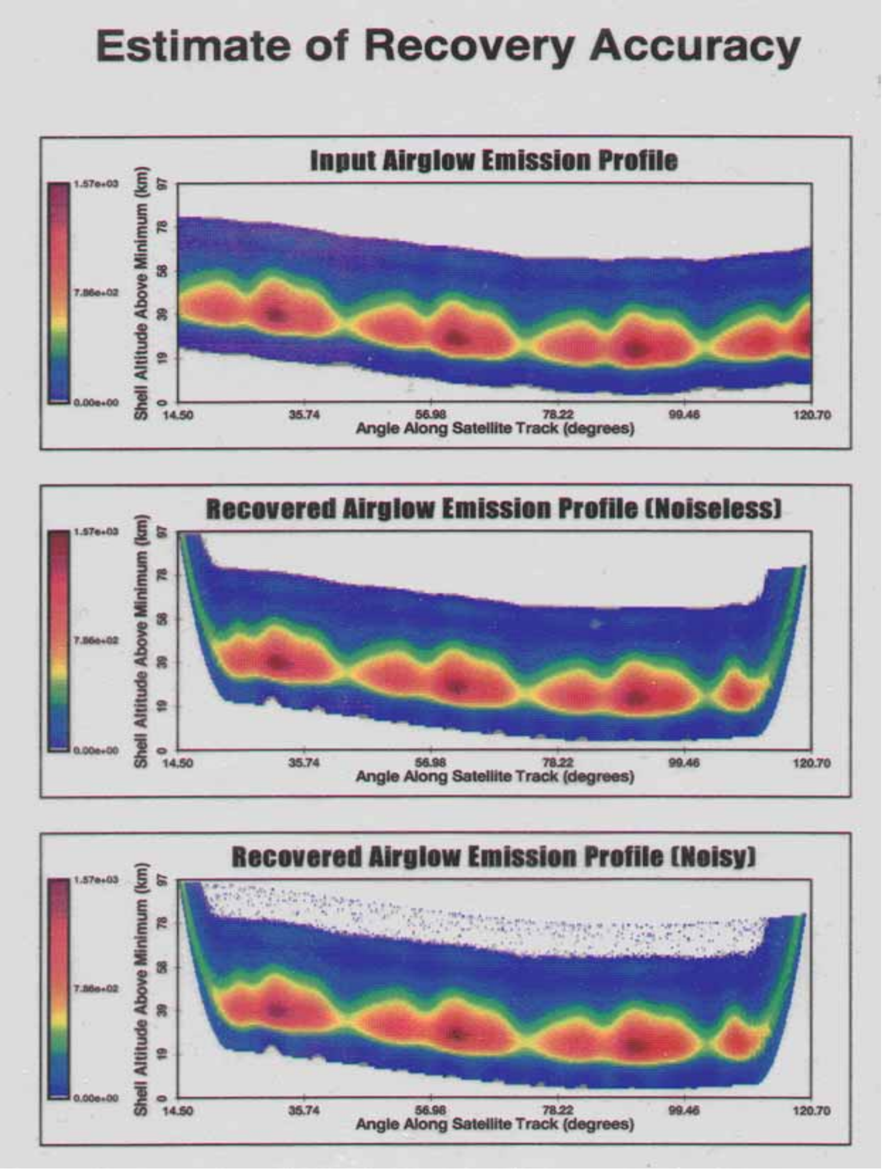

Model runs of the OSIRIS Tomography

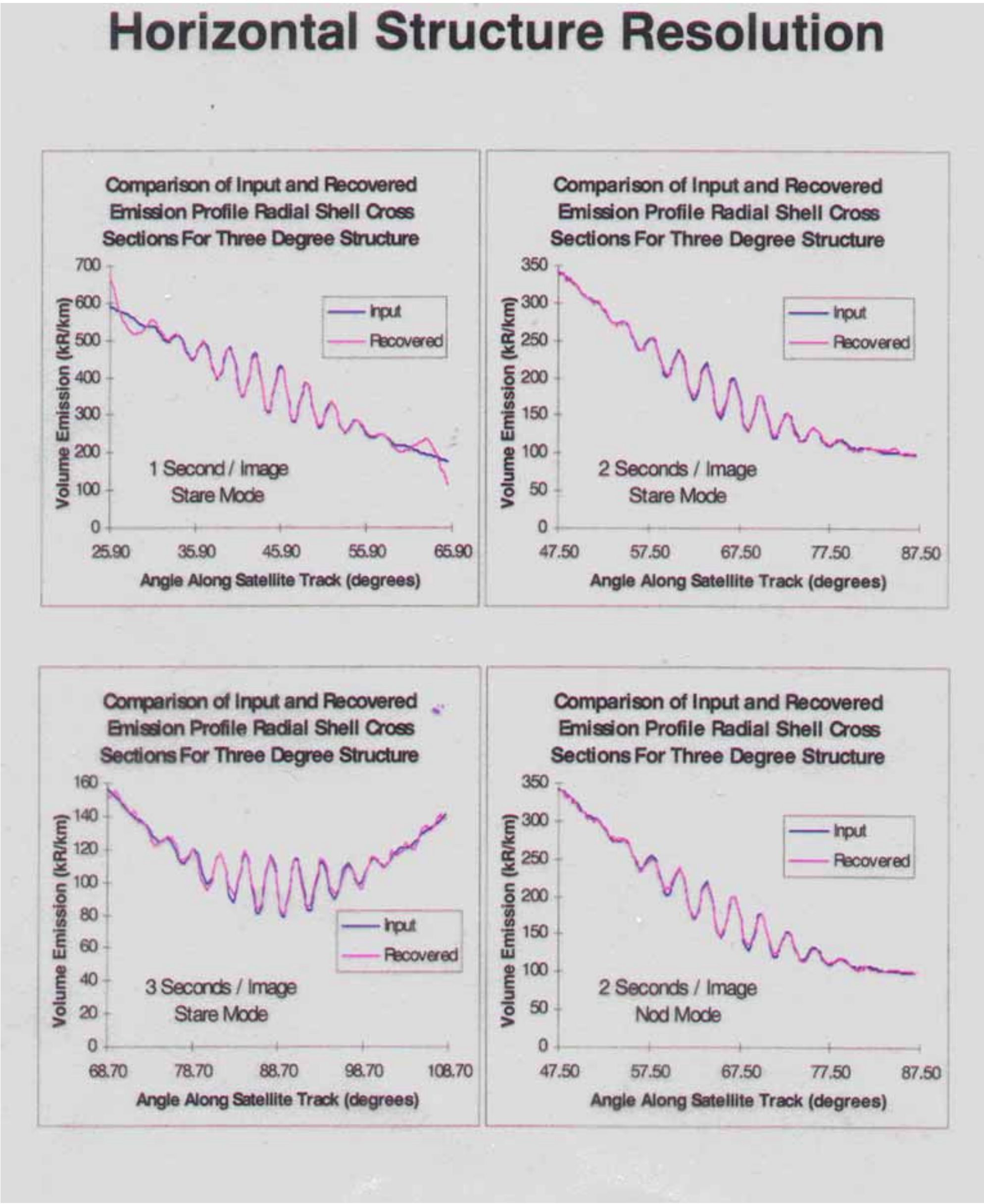

Model runs of the OSIRIS Tomography

Vertical Profiles

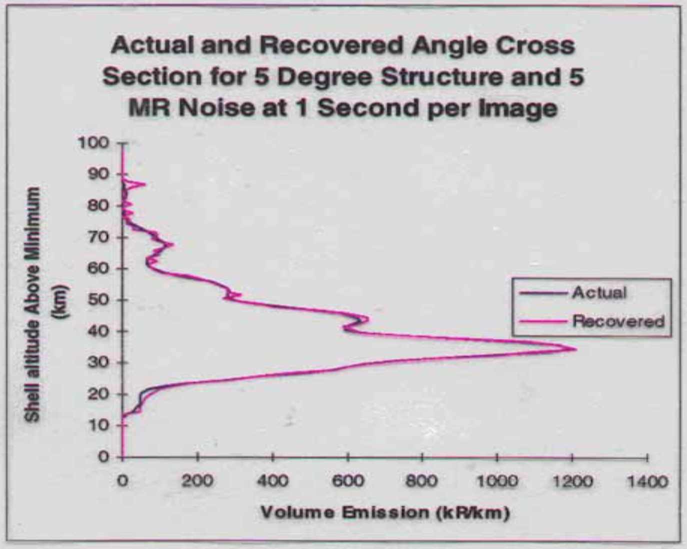

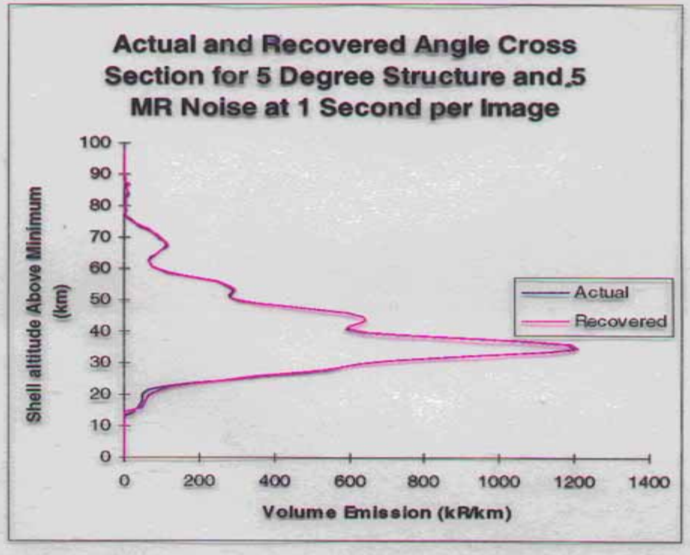

Typical Nighttime Limb Observations of the OH Airglow as seen with OSIRIS and the retrieved volume emission profile

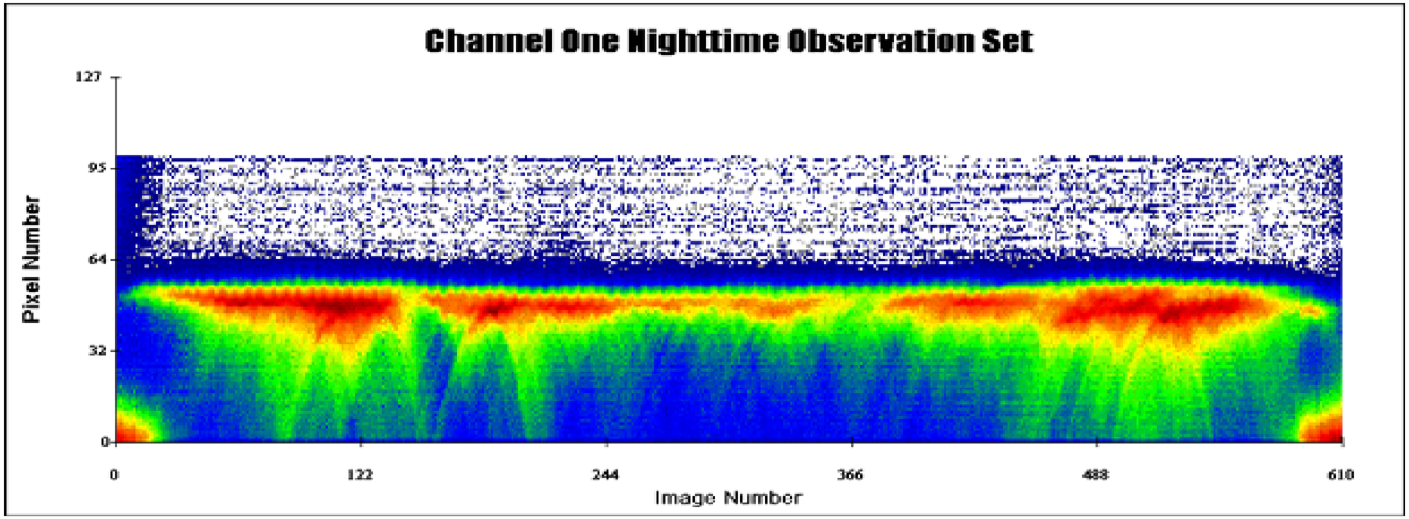

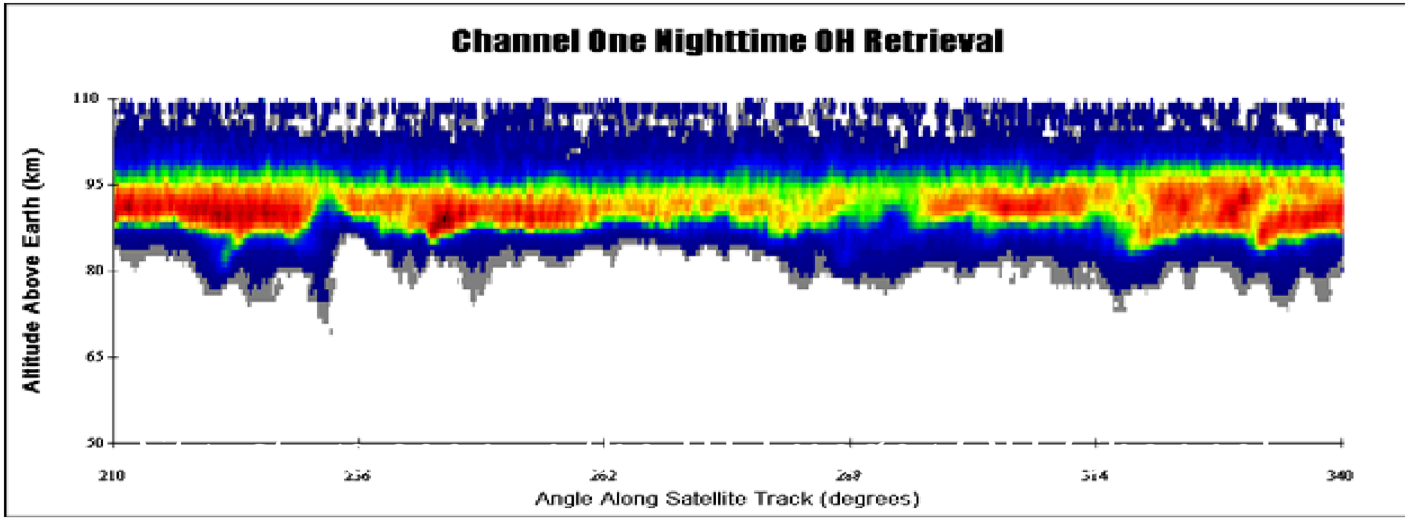

OSIRIS IRI Limb Observations of the OIRA Bands at 1.27μm

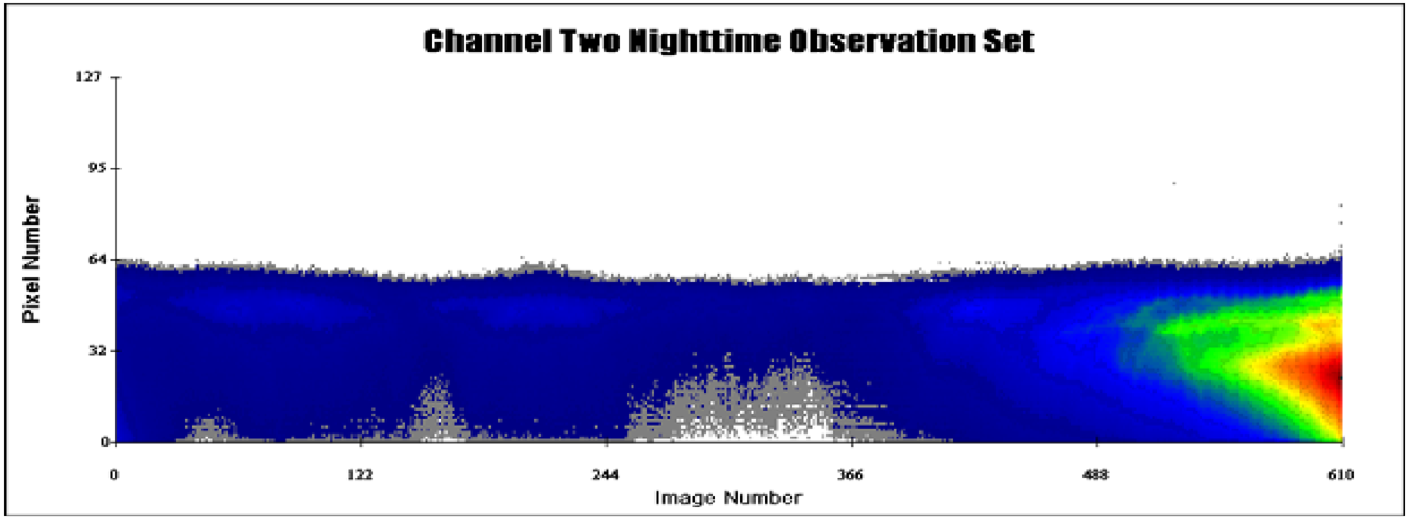

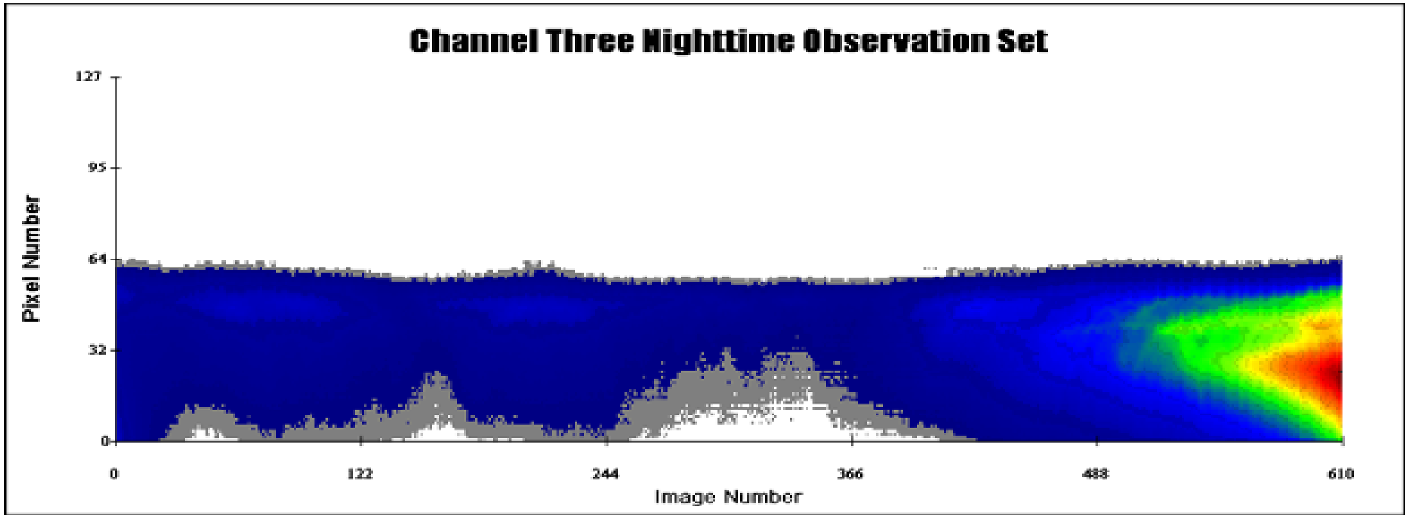

Inverted OSIRIS IRI Limb Observations of the OIRA Bands at 1.27μm

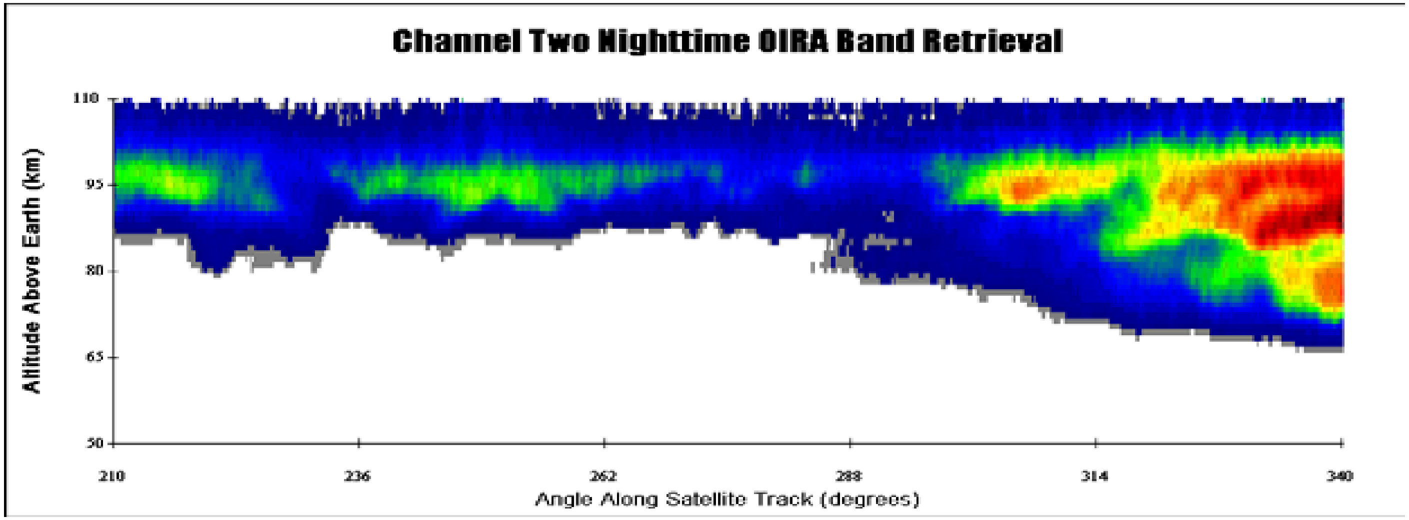

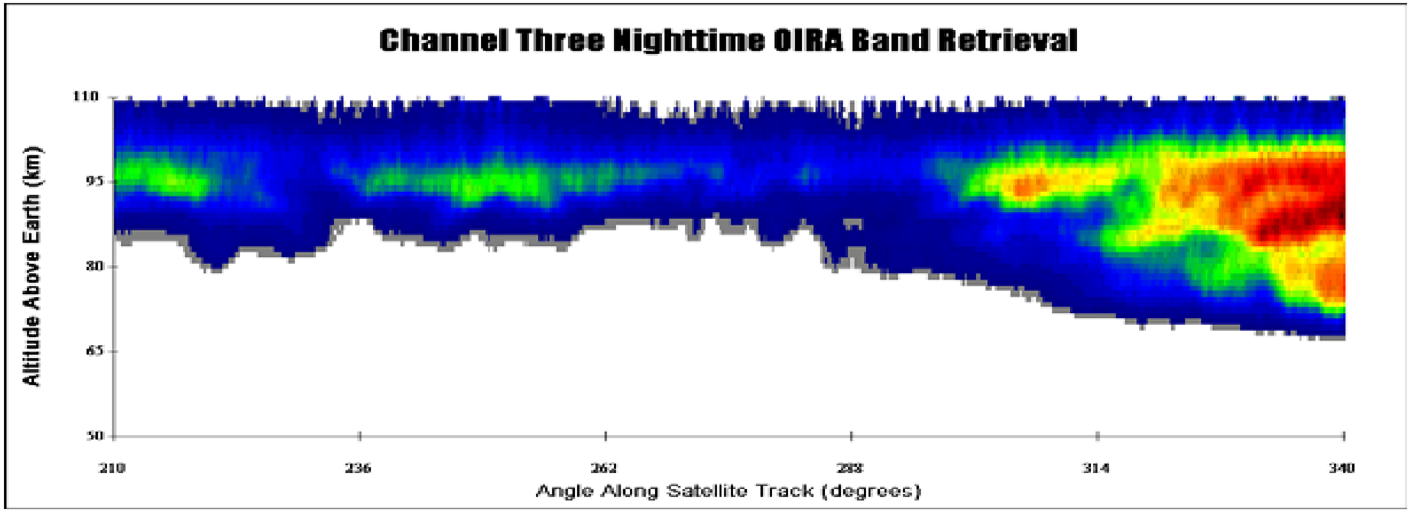

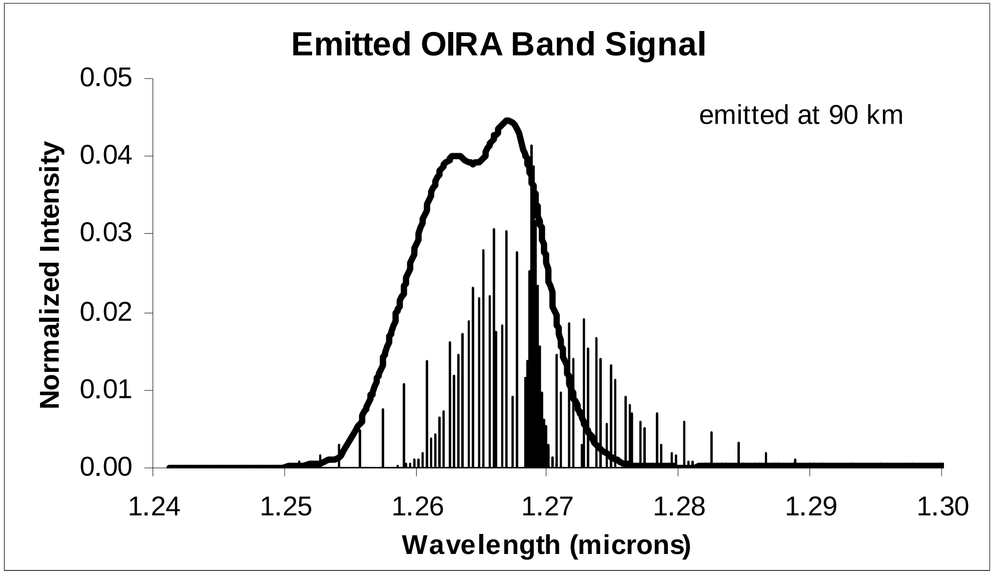

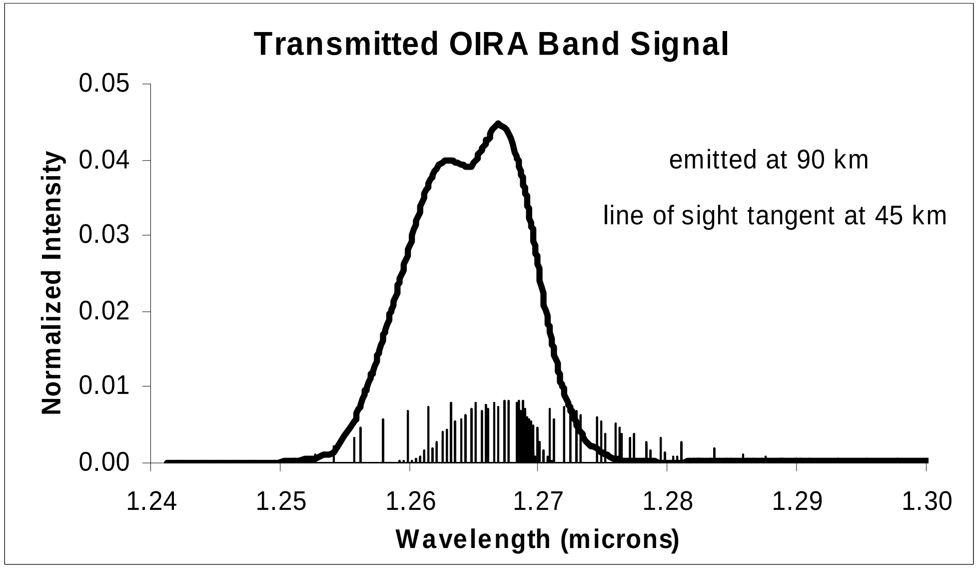

Emitted and Transmitted OIRA band as observed with OSIRIS. Filter band shape is the solid line, the spectrum is indicated by the stick plot.

Inverted OSIRIS IRI Limb Observations of the OH(3-1) Meinel Band.

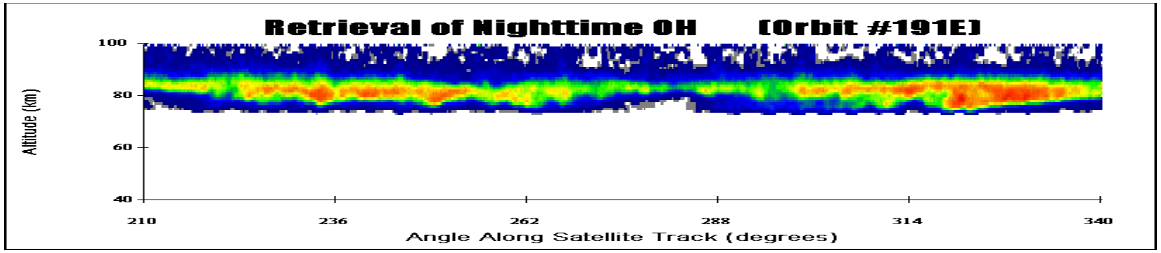

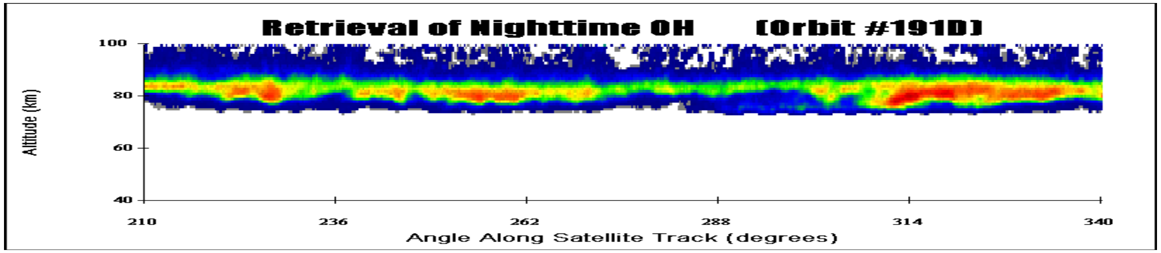

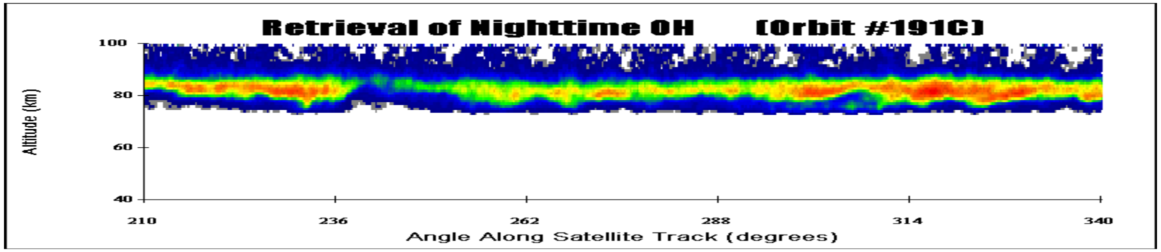

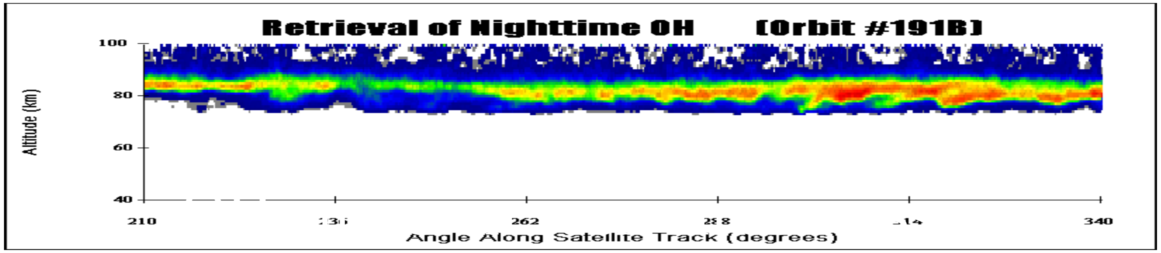

Daily average of the inverted OSIRIS IRI Limb Observations of the OH(3-1) Meinel Band.

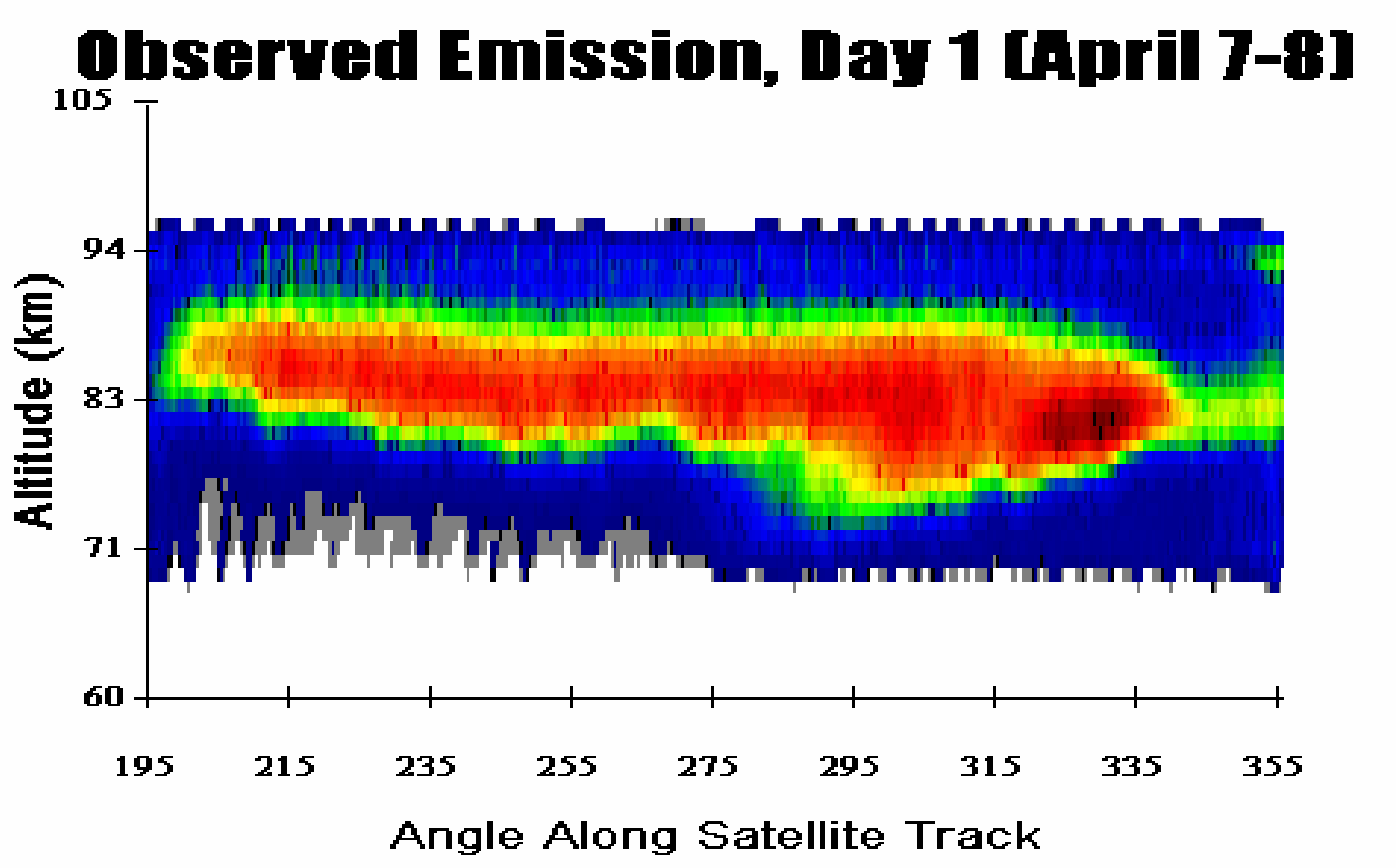

Daily average of the inverted OSIRIS IRI Limb Observations of the OH(3-1) Meinel Band.

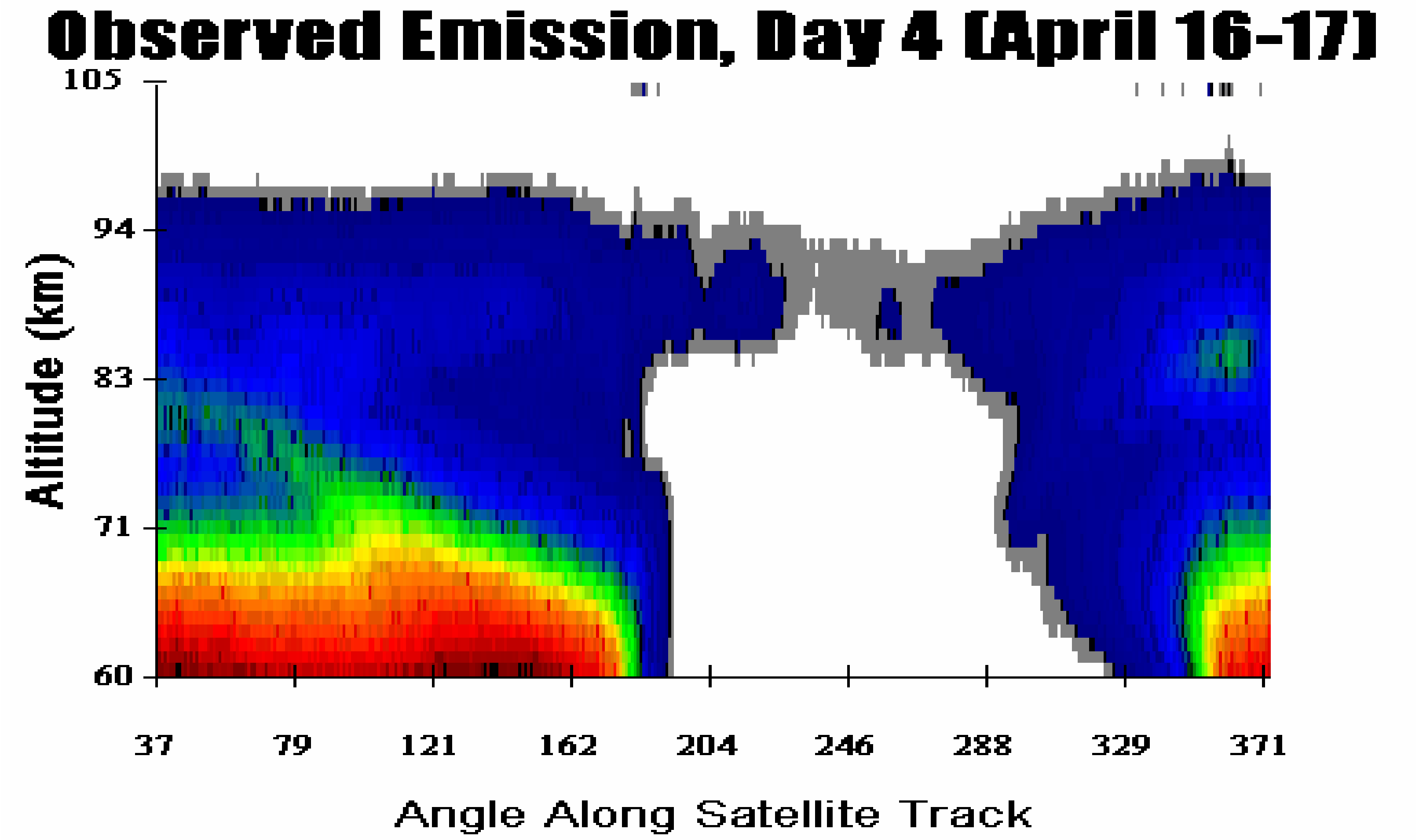

Daily average of the inverted OSIRIS IRI Limb Observations of the OH(3-1) Meinel Band.

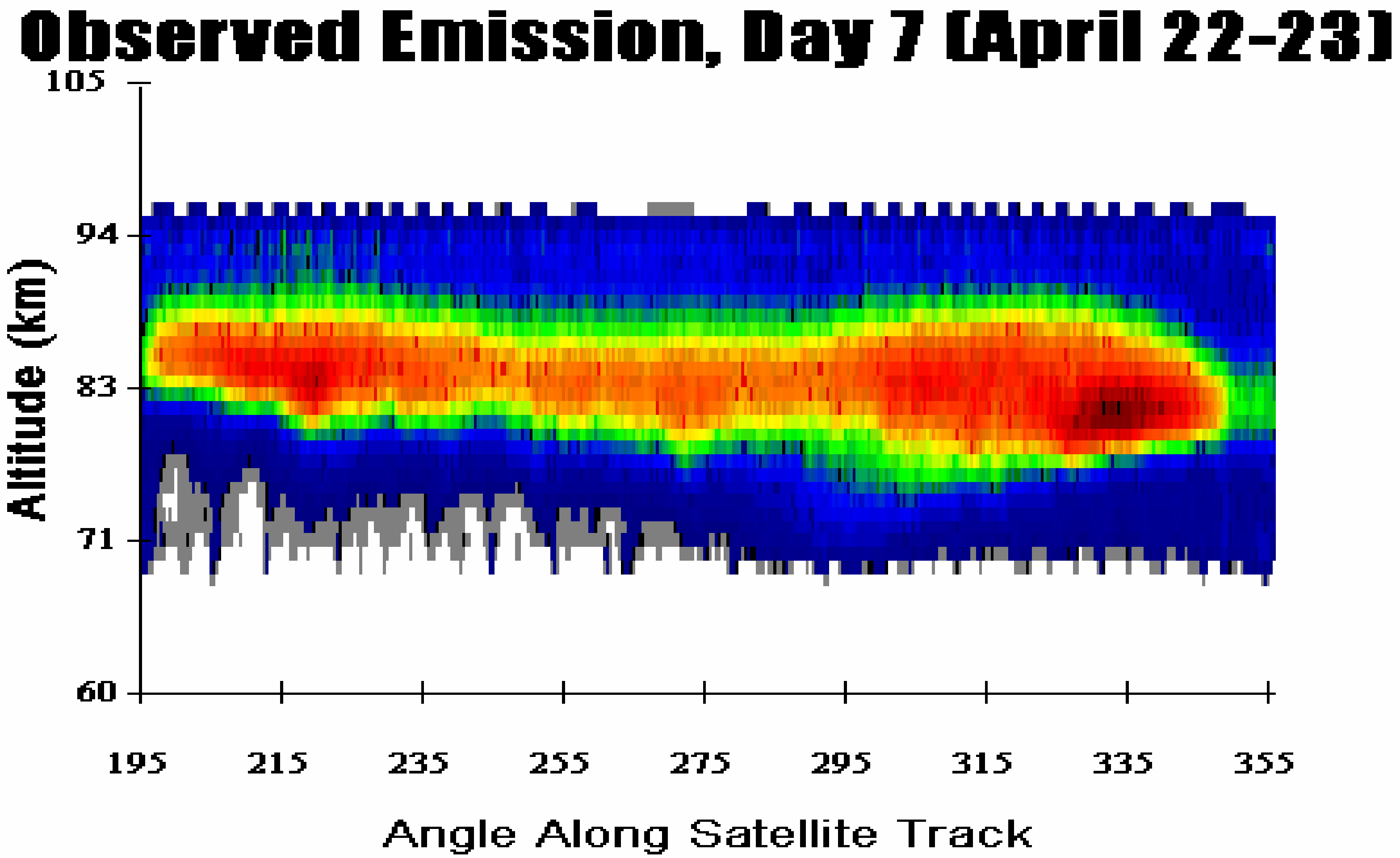

Daily average of the inverted OSIRIS IRI Limb Observations of the OH(3-1) Meinel Band.

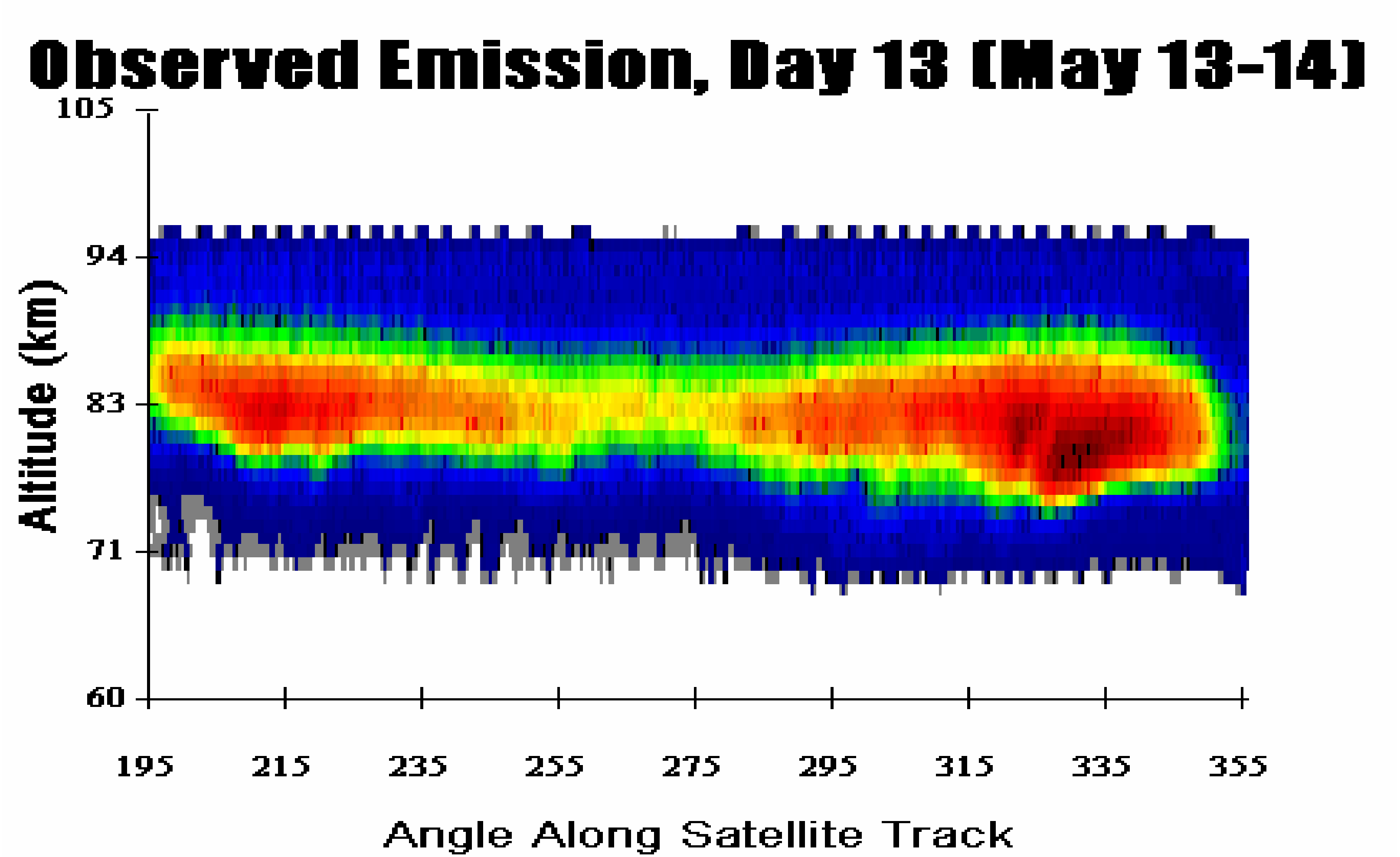

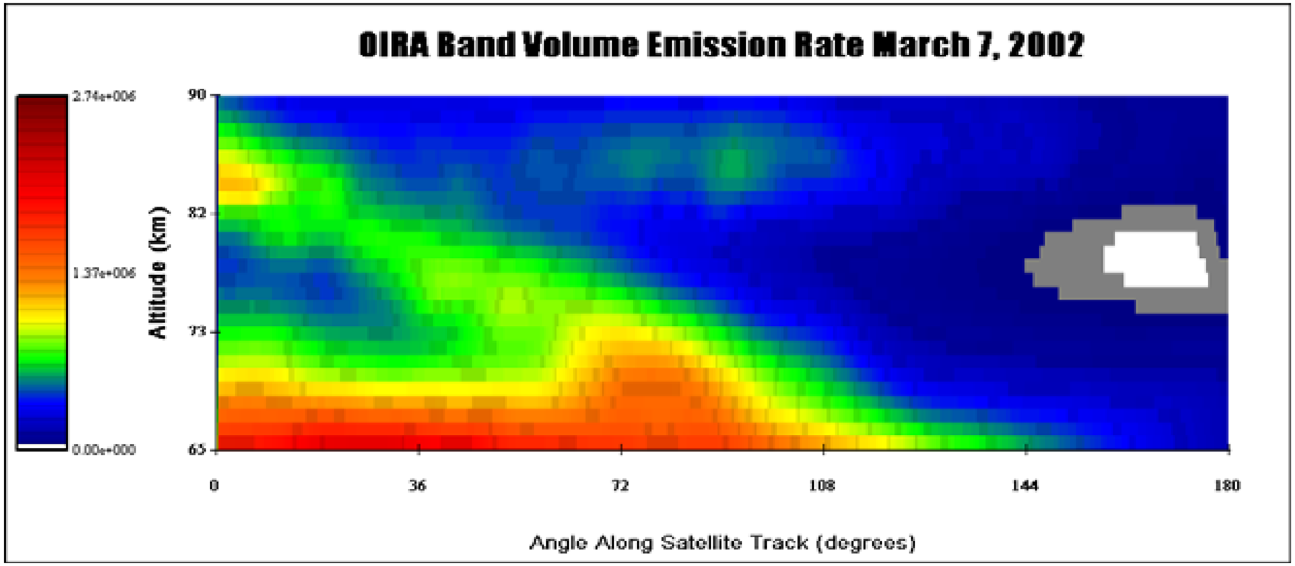
O1RA Band Volume Emission Rate March 7, 2002
2.74e+006
1.37e+006
0.00e+000
Altitude (km)
90
82
73
65
0
36
72
108
144
180
Angle Along Satellite Track (degrees)

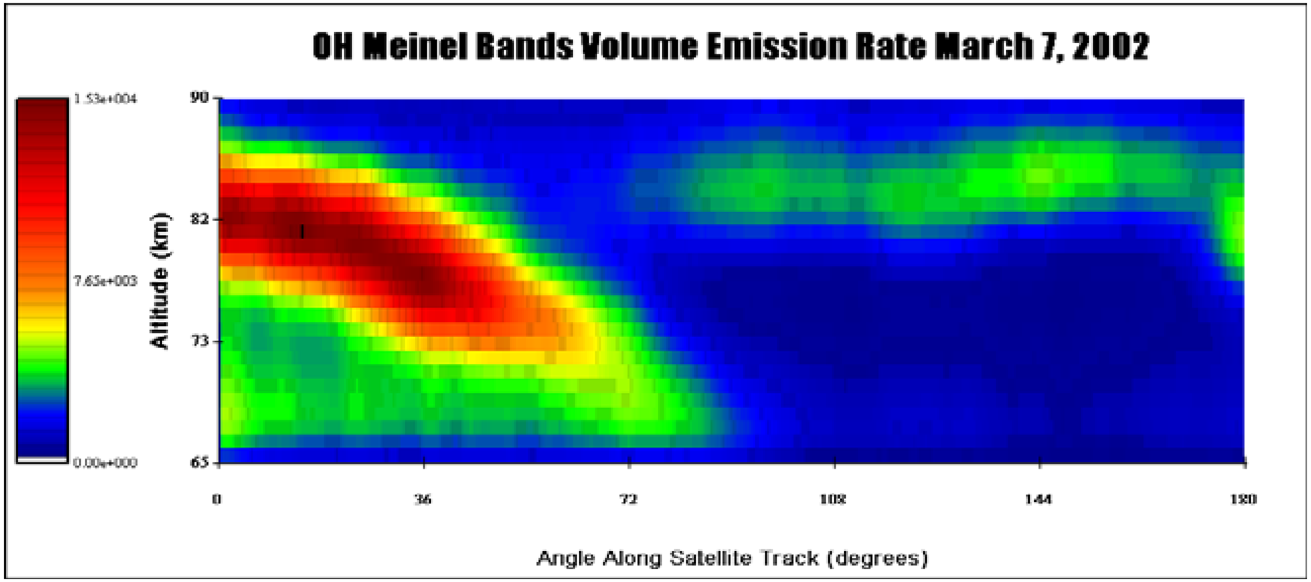
OH Meinel Bands Volume Emission Rate March 7, 2002
1.53e+004
7.65e+003
0.00e+000
Altitude (km)
90
82
73
65
0
36
72
108
144
180
Angle Along Satellite Track (degrees)

Details of the inverted OSIRIS IRI Limb Observations of the OIRA Bands at 1.27μm

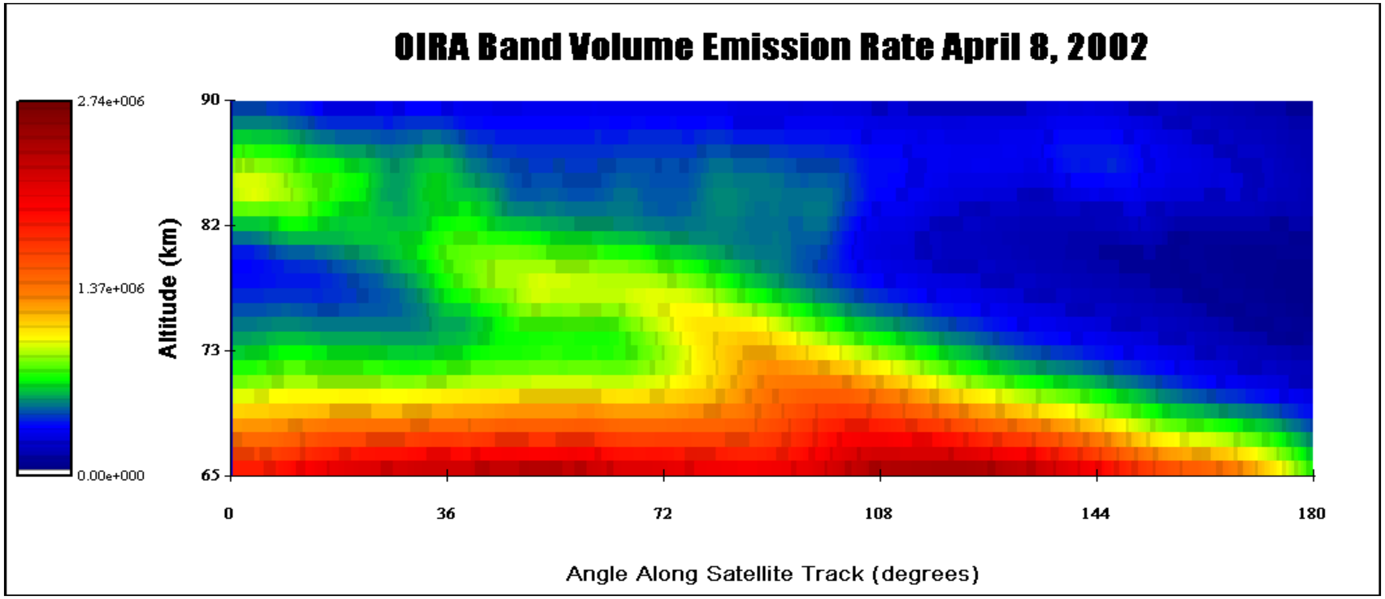

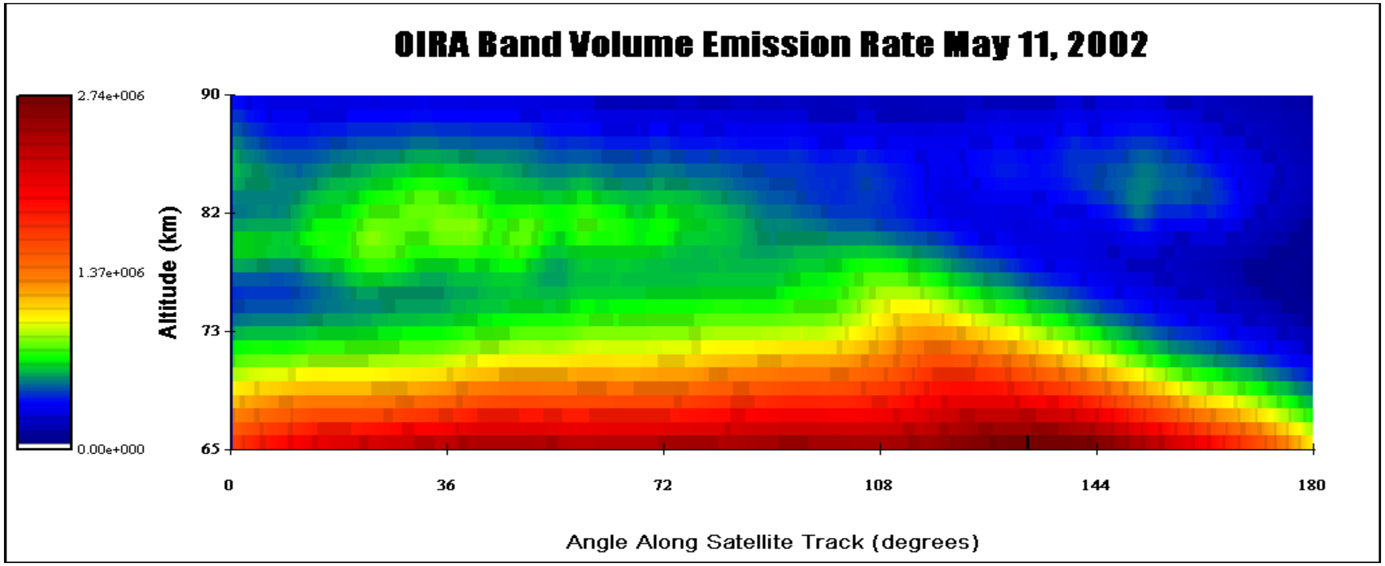

Details of the inverted OSIRIS IRI Limb Observations of the OIRA Bands at 1.27μm

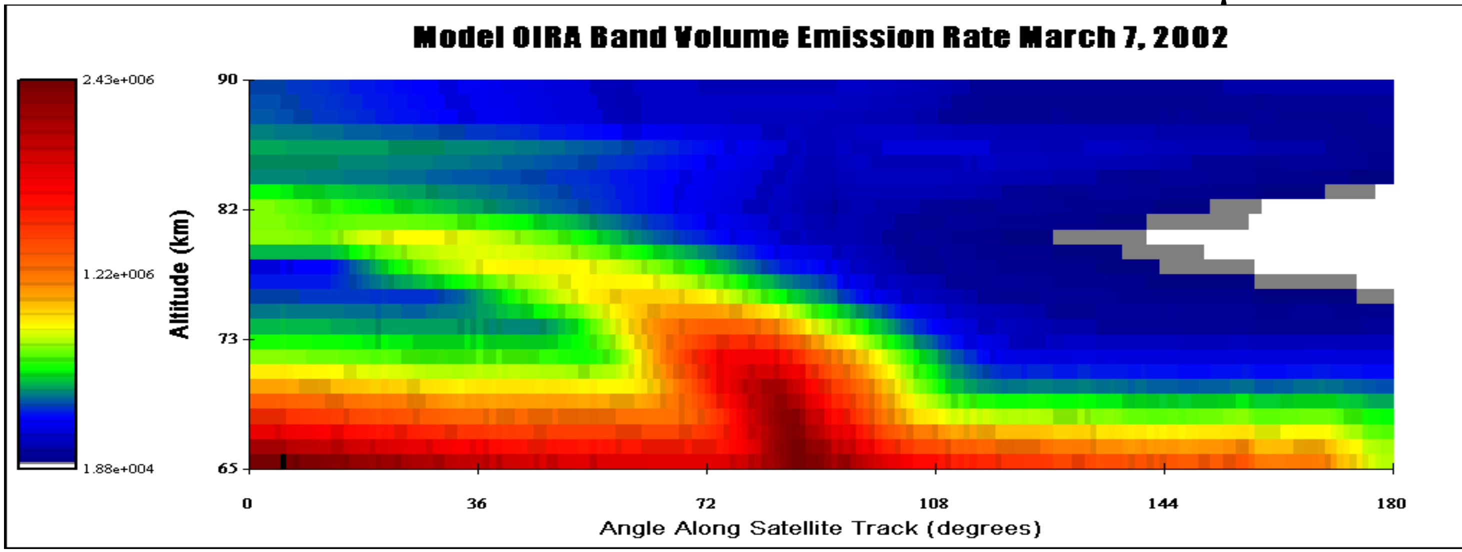

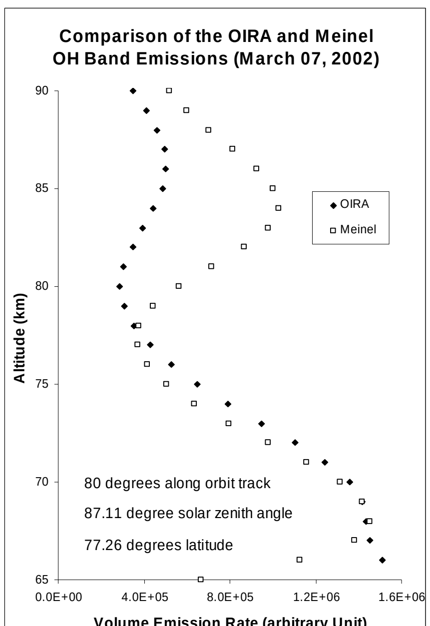

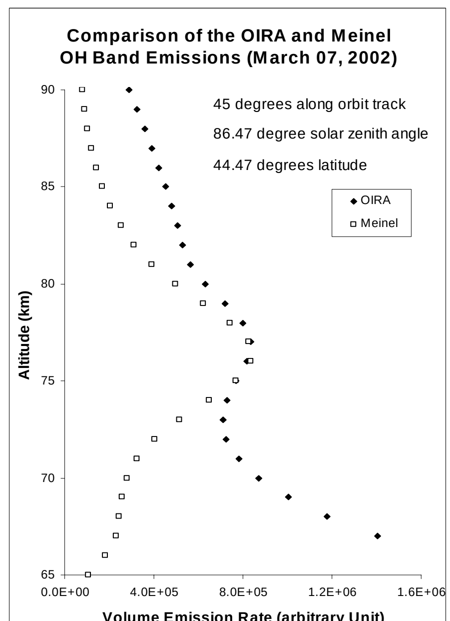

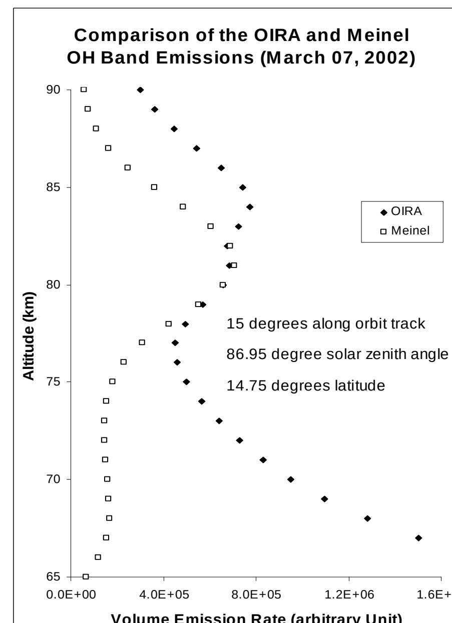

Details of the inverted OSIRIS IRI Limb Observations of the OIRA Bands at 1.27μm during the Halloween Storm 2003.

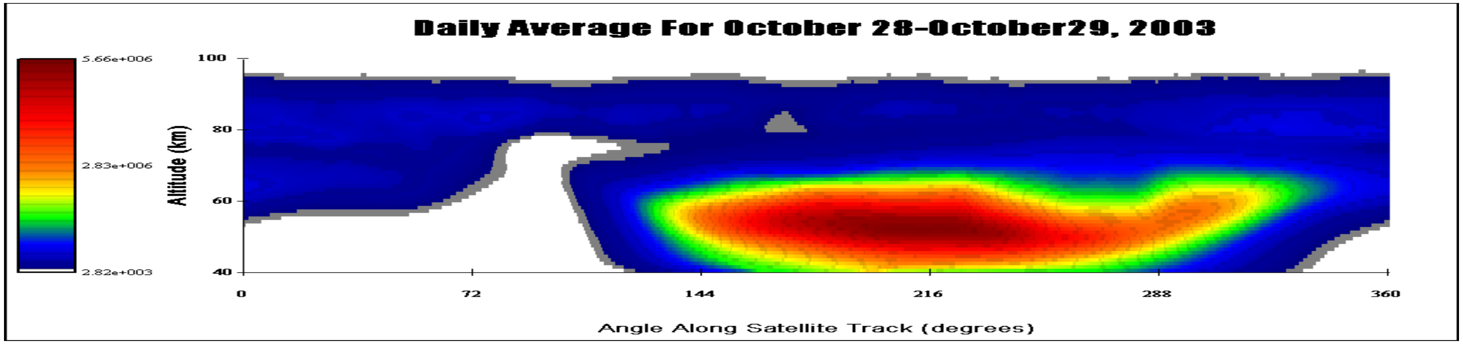

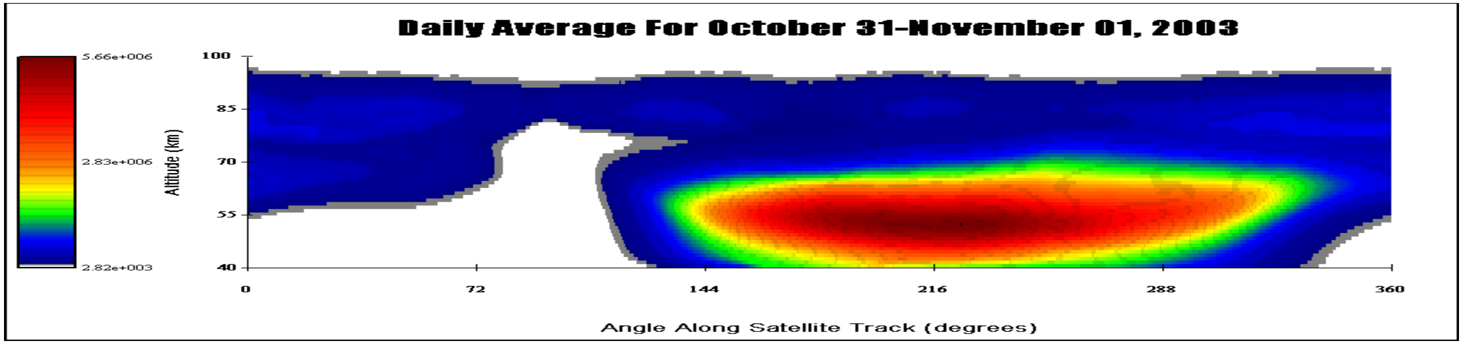

Details of the inverted OSIRIS IRI Limb Observations of the OIRA Bands at 1.27μm during the Halloween Storm 2003.

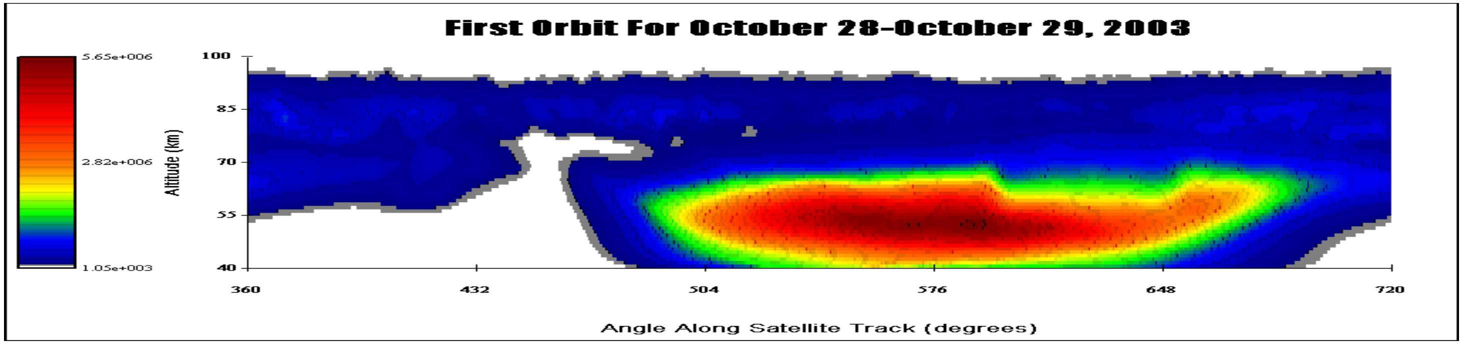

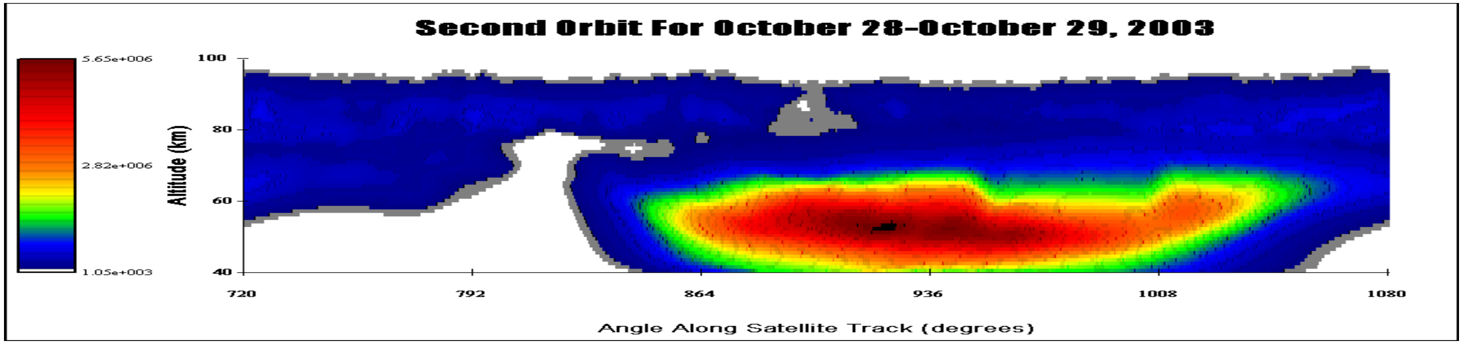

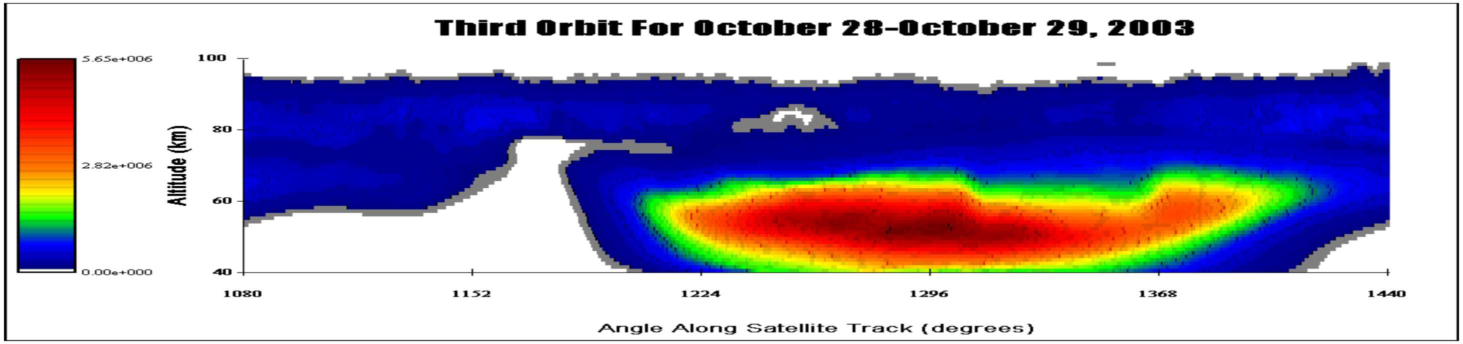

Details of the inverted OSIRIS IRI Limb Observations of the OIRA Bands at 1.27μm during the Halloween Storm 2003.

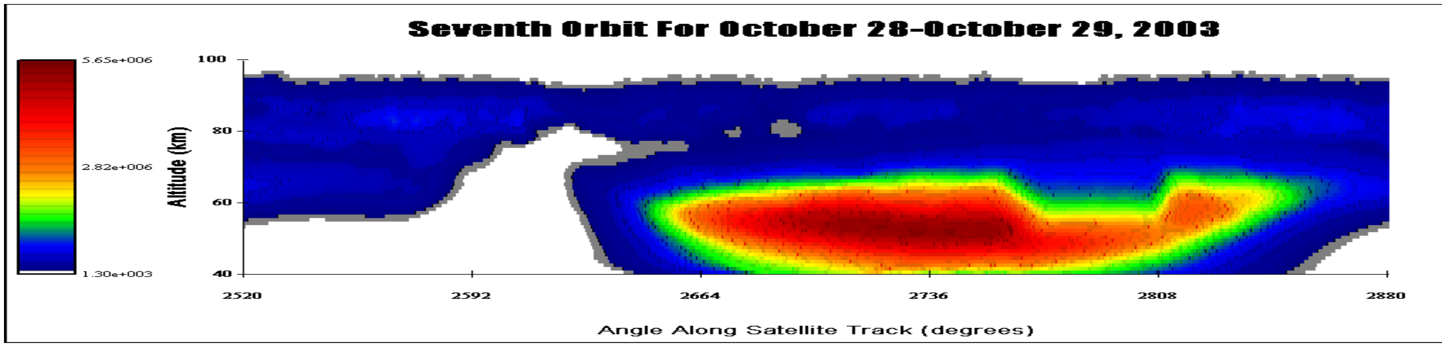

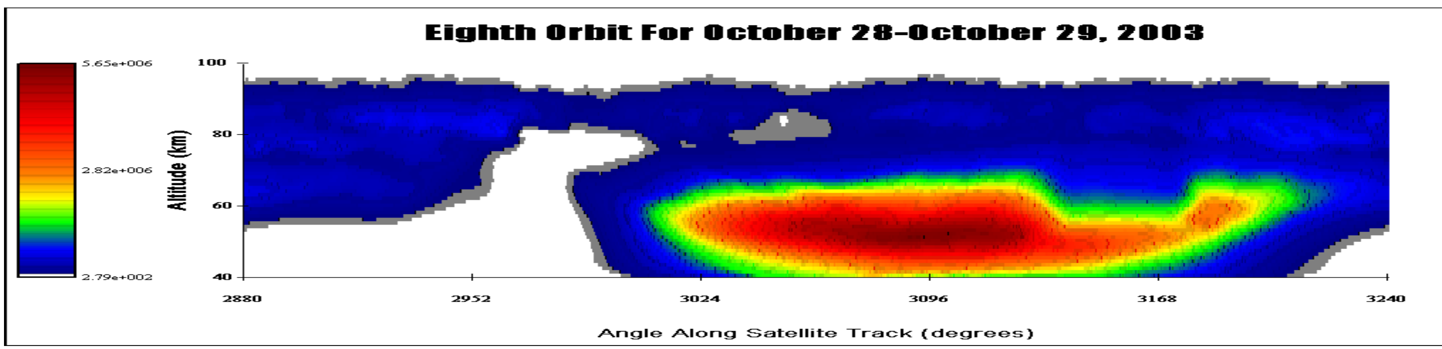

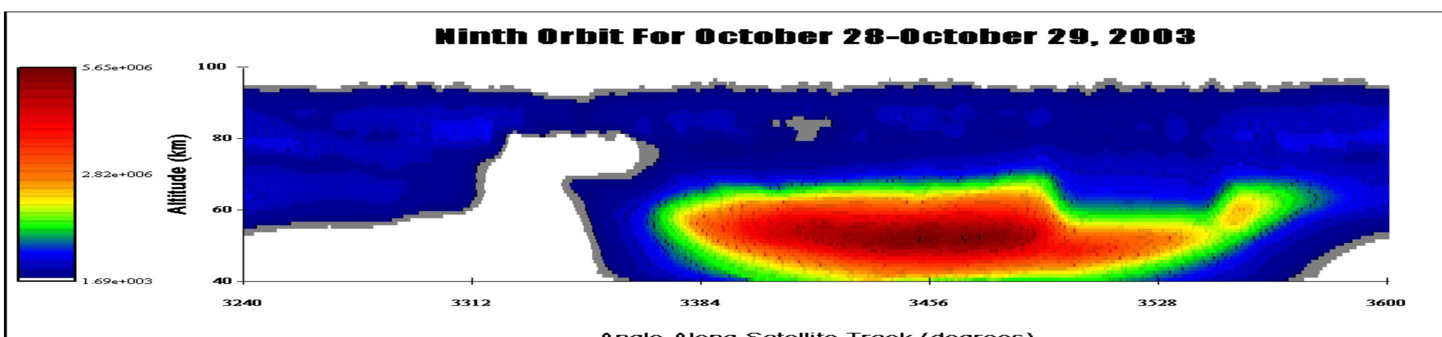

Details of the inverted OSIRIS IRI Limb Observations of the OIRA Bands at 1.27μm during the Halloween Storm 2003.

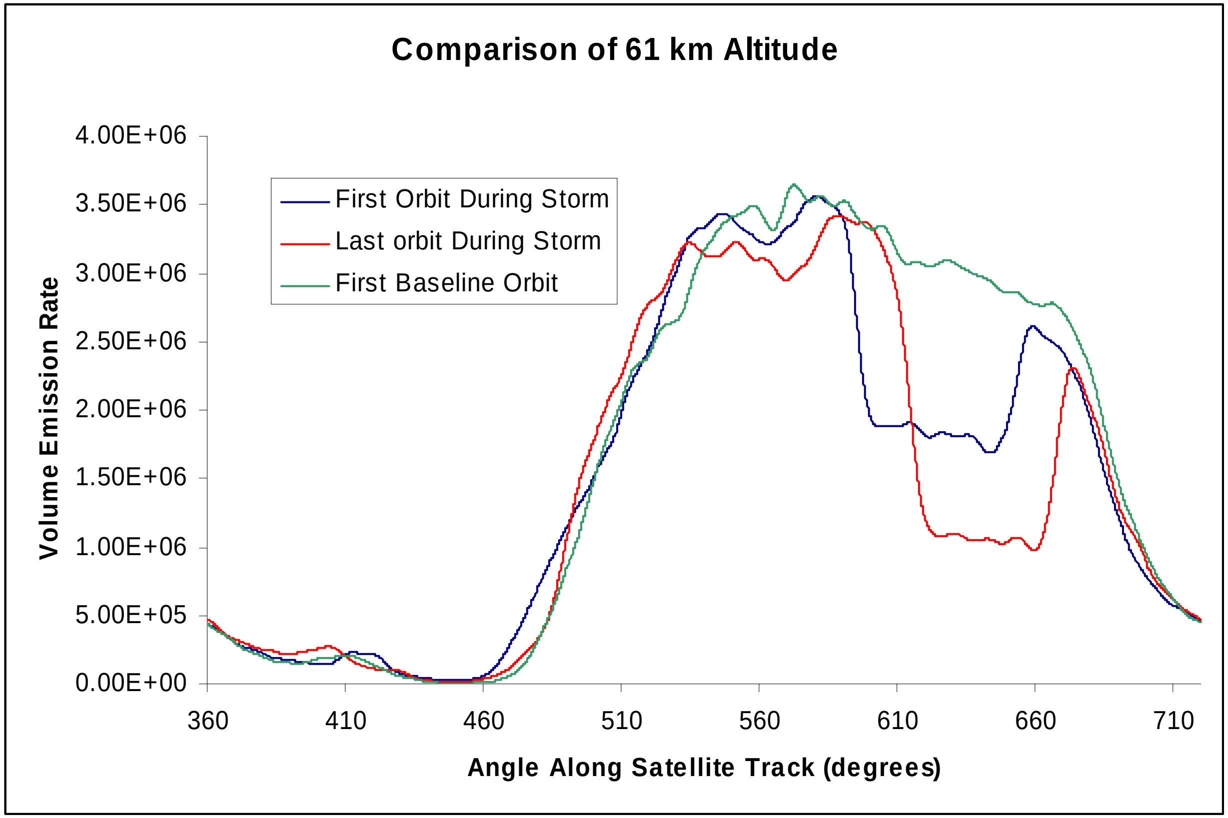

Details of the inverted OSIRIS IRI Limb Observations of the OIRA Bands at 1.27μm during the Halloween Storm 2003.

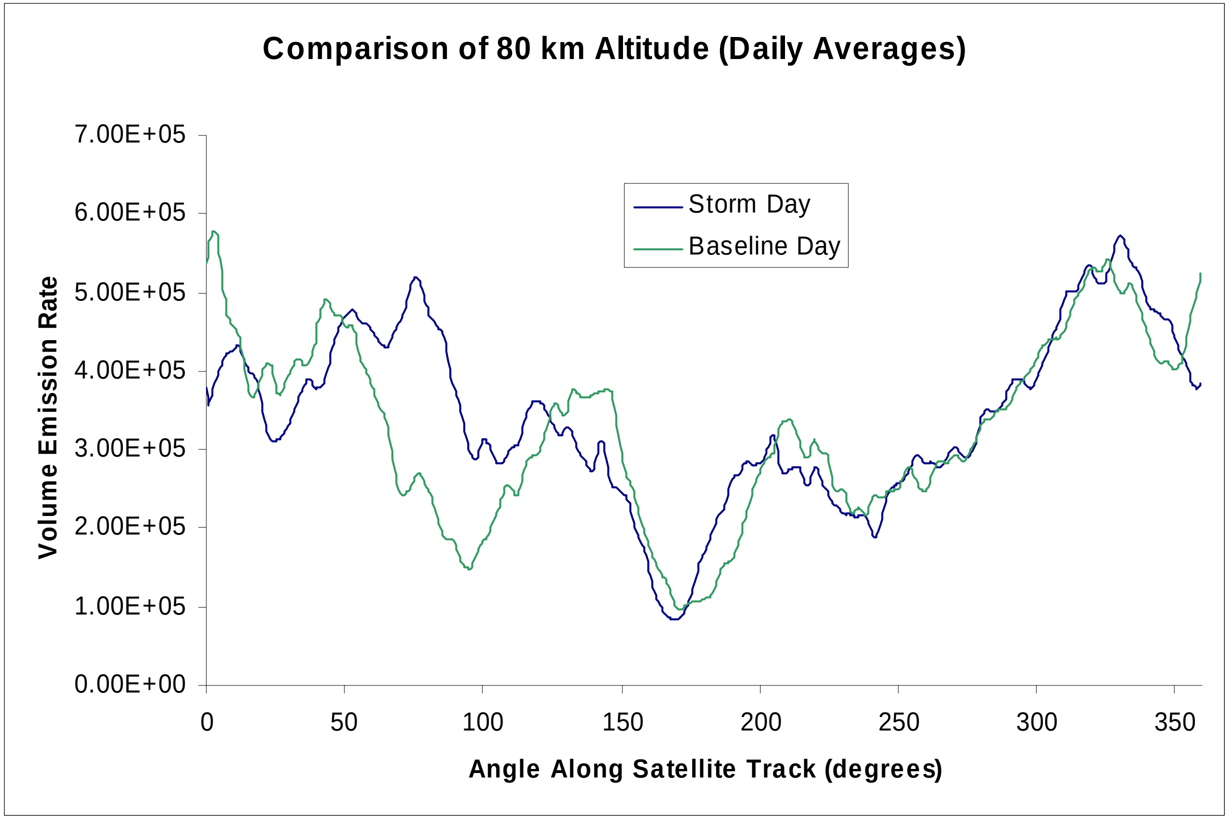

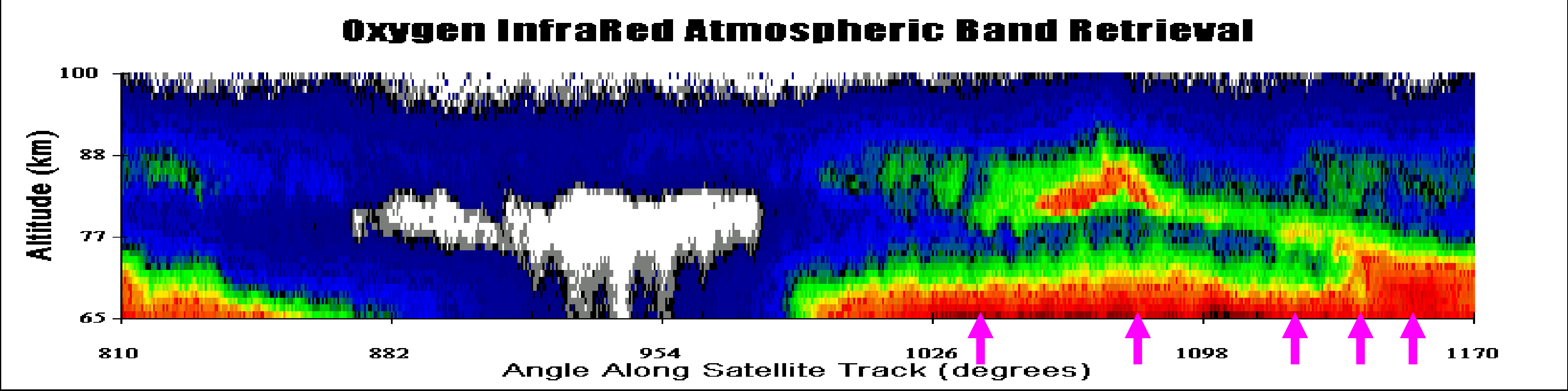
Oxygen InfraRed Atmospheric Band Retrieval
Altitude (km)
100
88
77
65
810
882
954
1026
1098
1170
Angle Along Satellite Track (degrees)

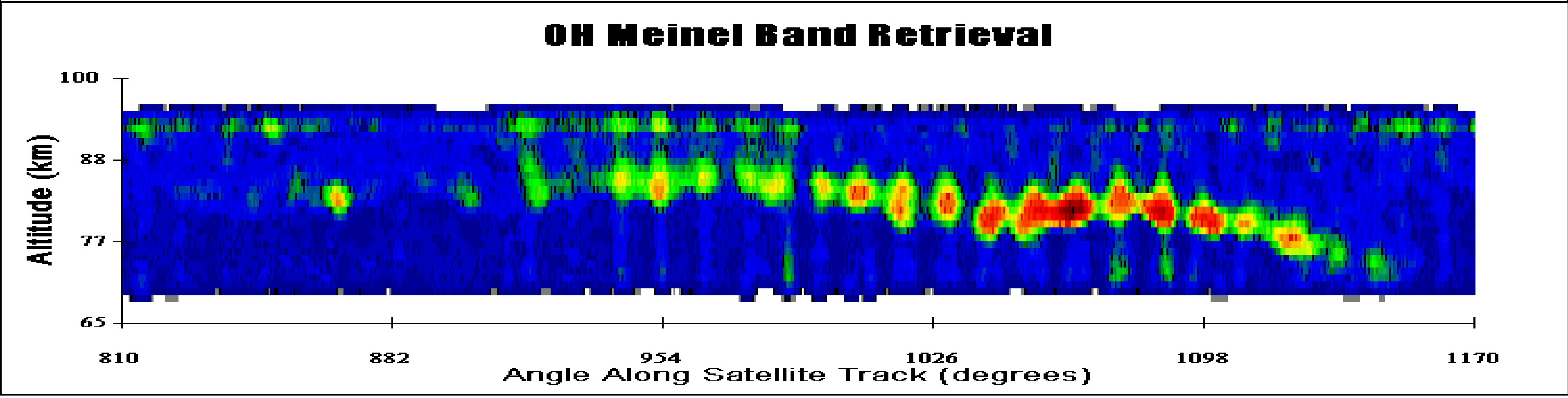
OH Meinel Band Retrieval
Altitude (km)
100
88
77
65
810
882
954
1026
1098
1170
Angle Along Satellite Track (degrees)

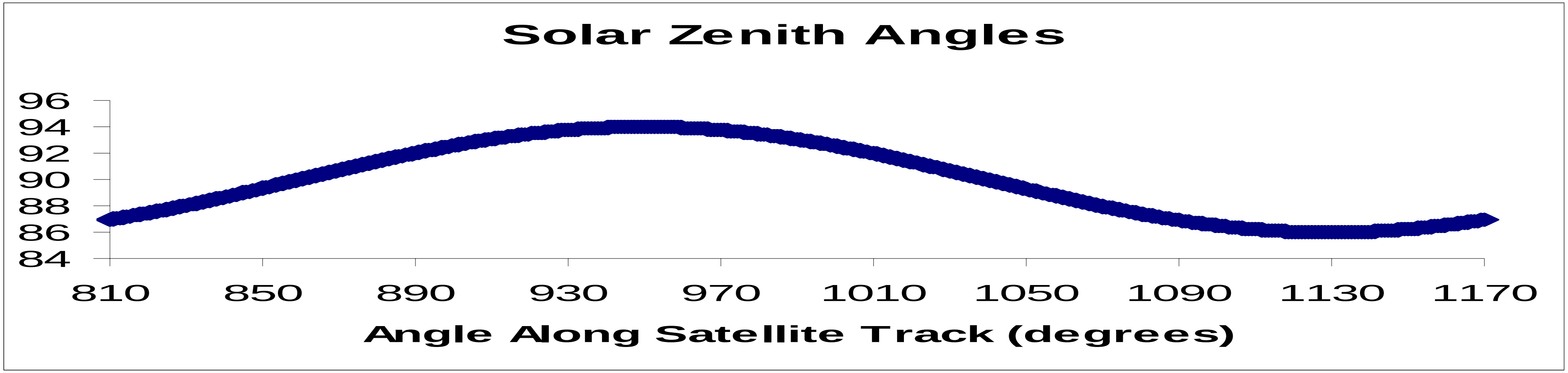
Solar Zenith Angles
96
94
92
90
88
86
84
810
850
890
930
970
1010
1050
1090
1130
1170
Angle Along Satellite Track (degrees)

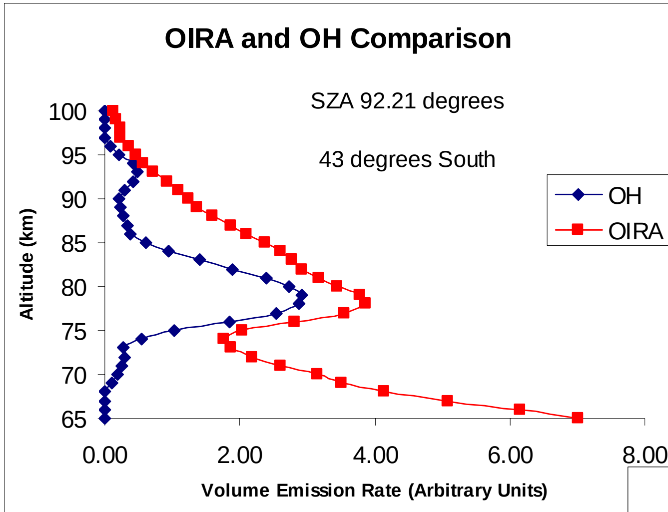
OIRA and OH Comparison
SZA 92.21 degrees
43 degrees South
OH
OIRA
Altitude (km)
Volume Emission Rate (Arbitrary Units)

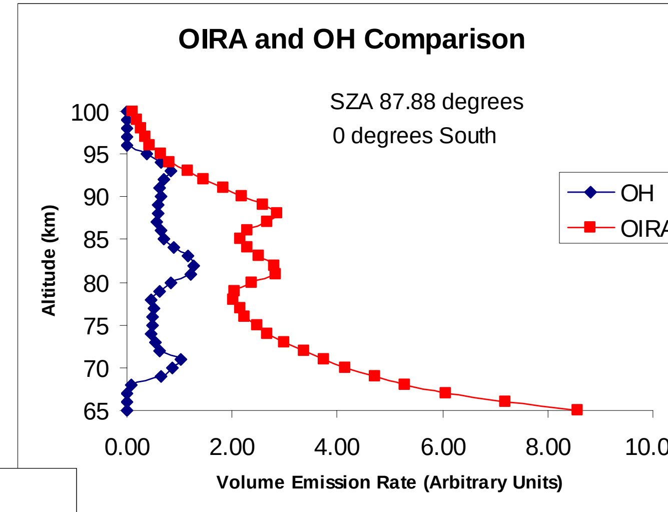
OIRA and OH Comparison
SZA 87.88 degrees
0 degrees South
OH
OIRA
Altitude (km)
Volume Emission Rate (Arbitrary Units)

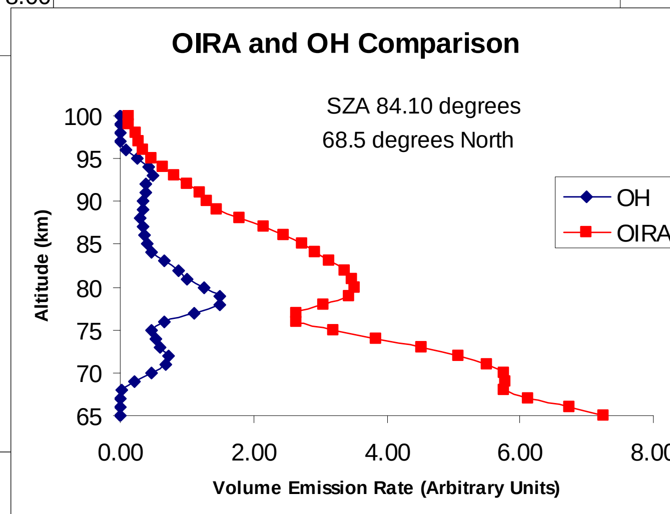
OIRA and OH Comparison
SZA 84.10 degrees
68.5 degrees North
OH
OIRA
Altitude (km)
Volume Emission Rate (Arbitrary Units)

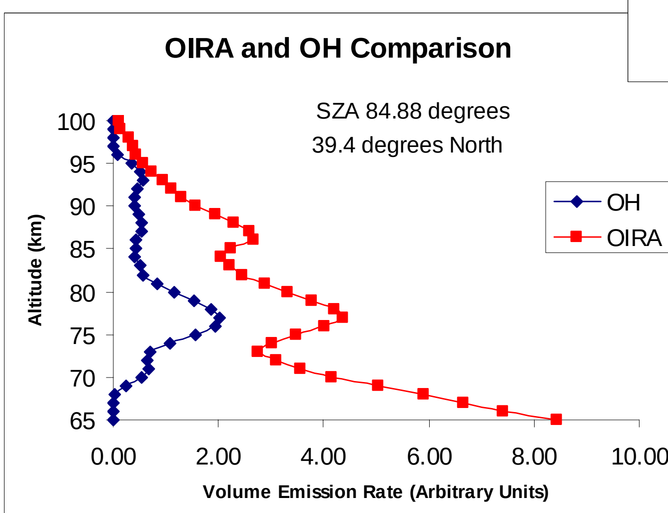
OIRA and OH Comparison
SZA 84.88 degrees
39.4 degrees North
OH
OIRA
Altitude (km)
Volume Emission Rate (Arbitrary Units)

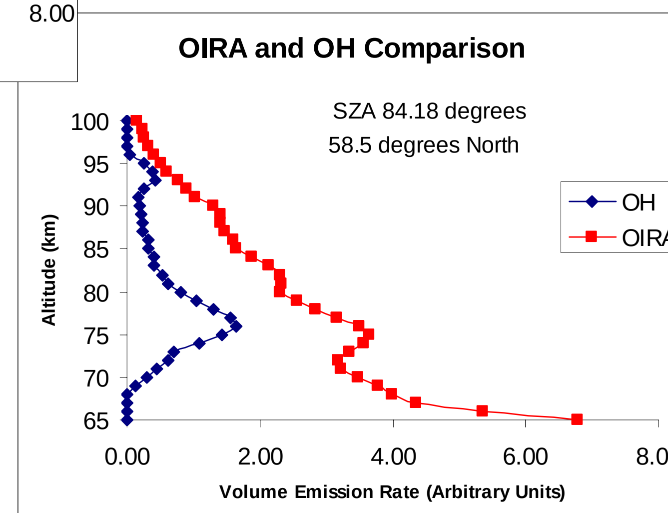
OIRA and OH Comparison
SZA 84.18 degrees
58.5 degrees North
OH
OIRA
Altitude (km)
Volume Emission Rate (Arbitrary Units)

Details of the height profiles derived from the inverted OSIRIS IRI Limb Observations.

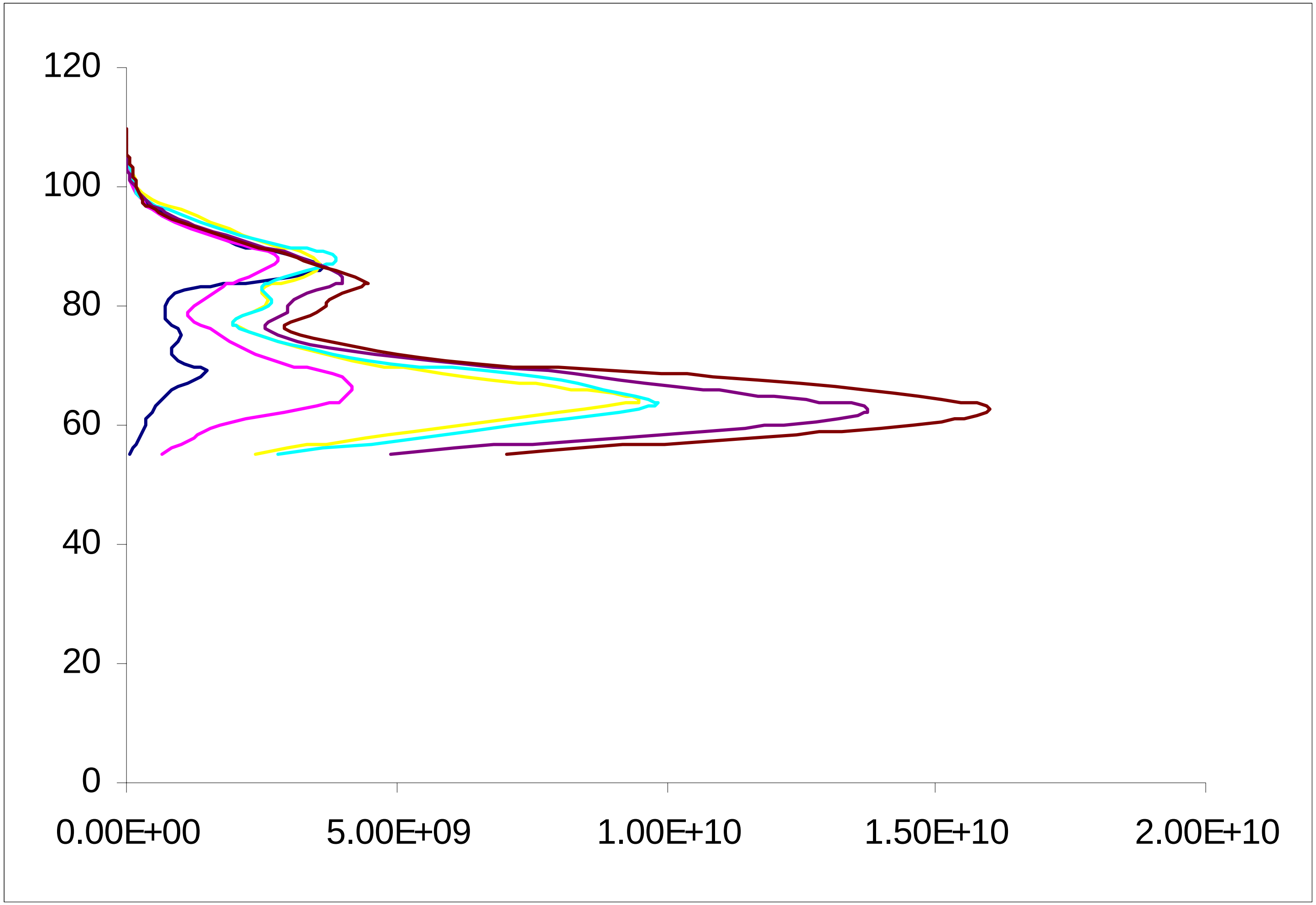

The measured overhead profile.

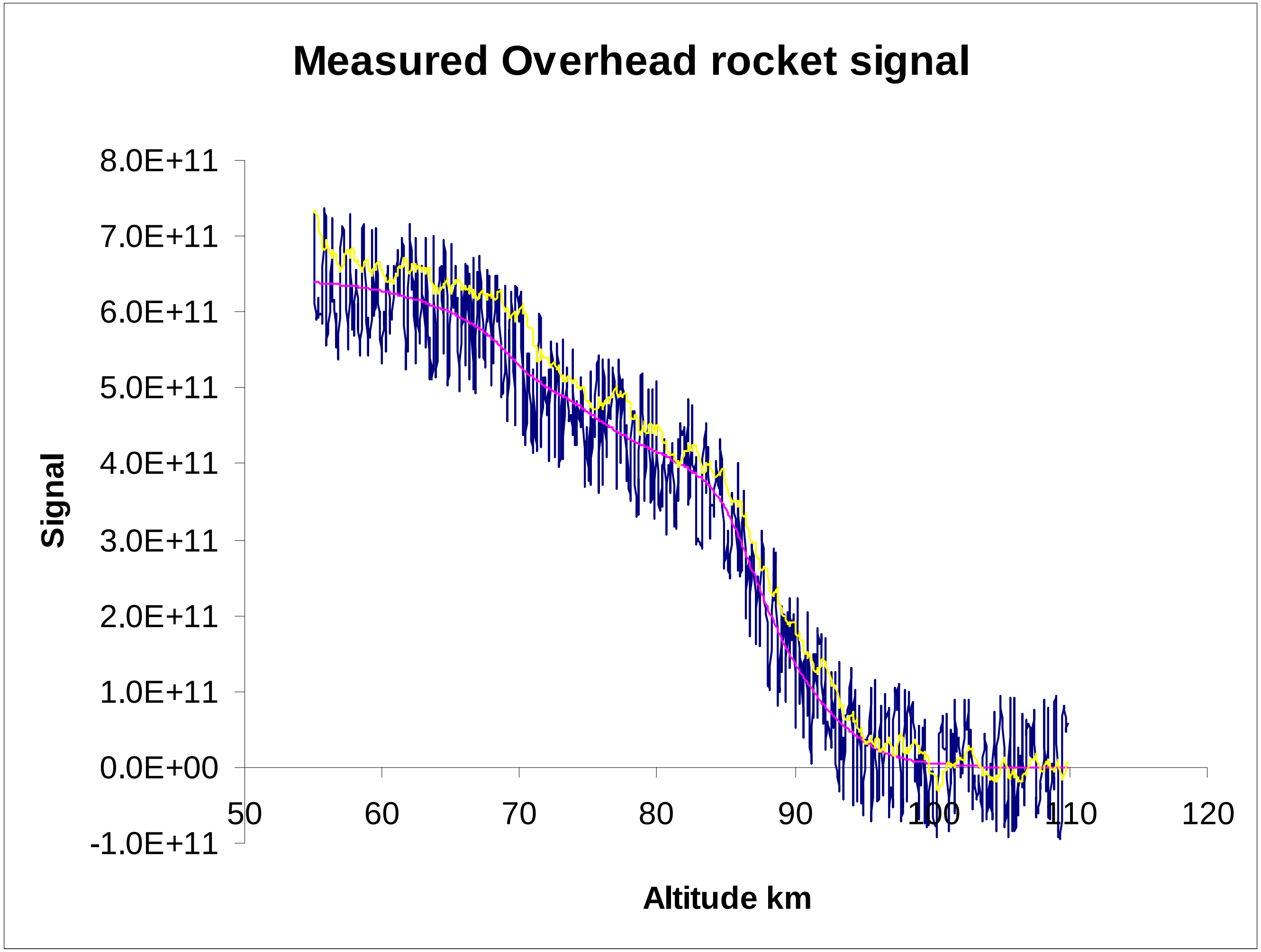

The derived height profile from the overhead measurements.

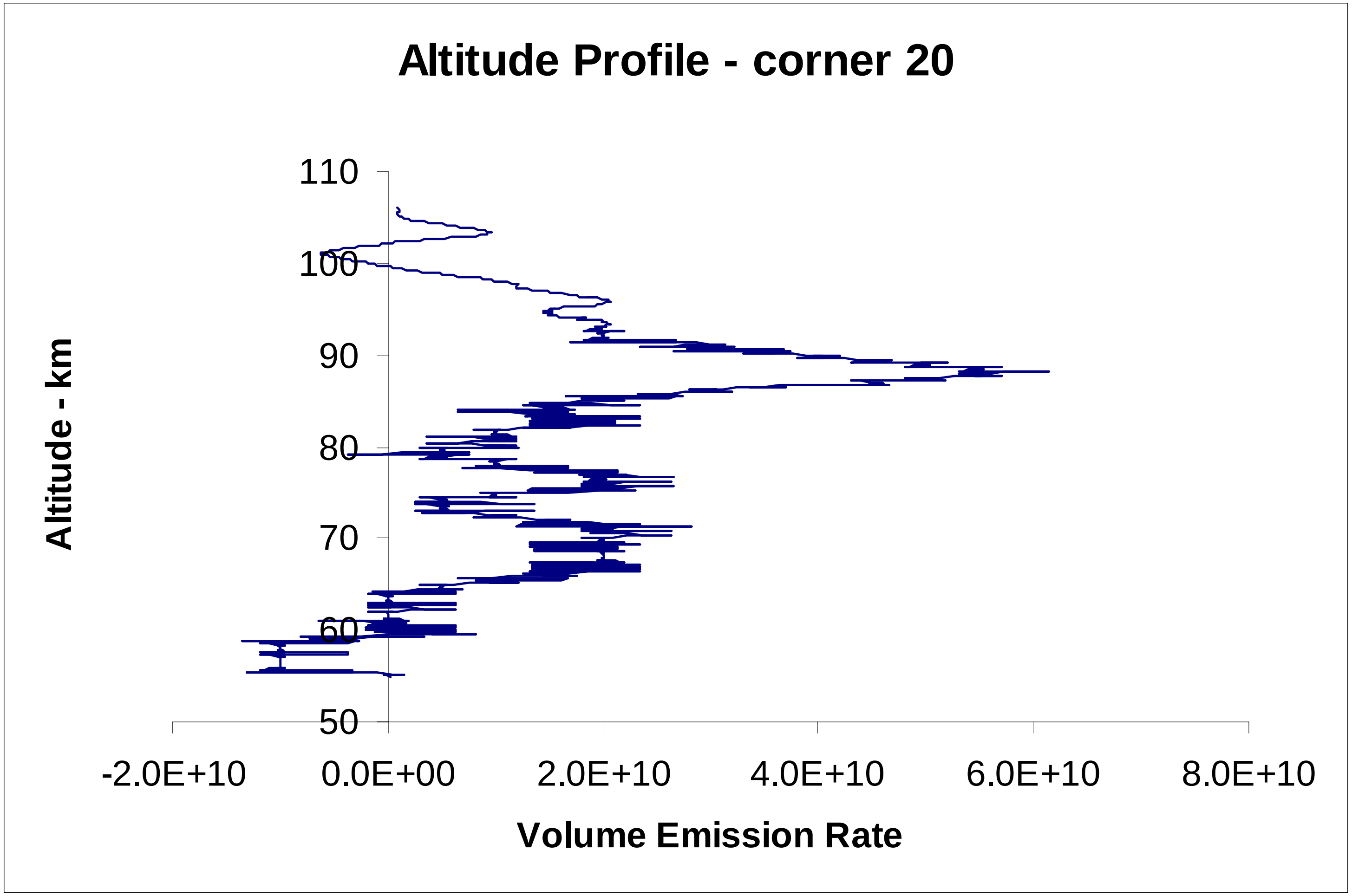

The derived height profile from the overhead measurements.

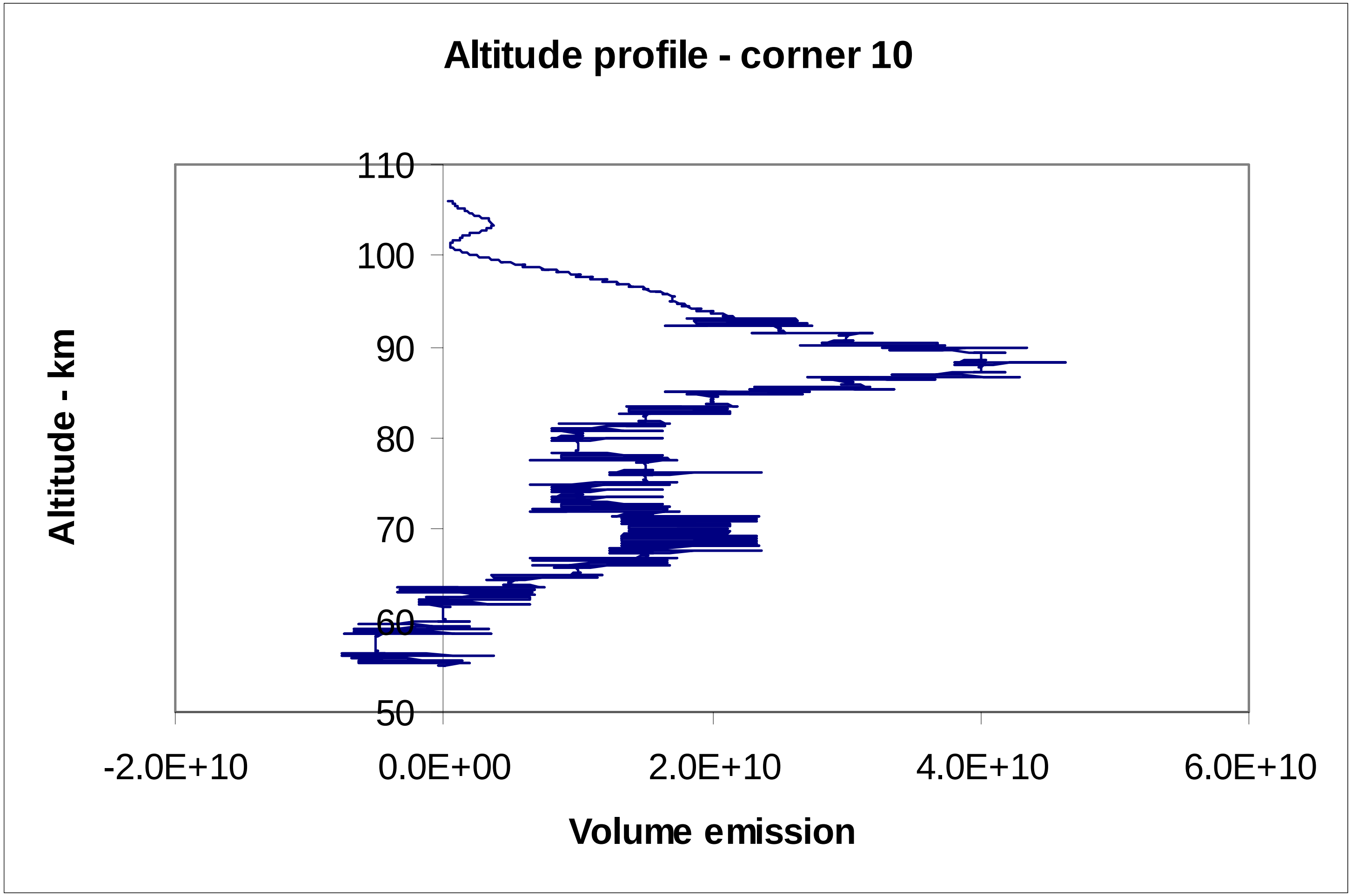

Imager Observations of the Atmosphere at 1.53 μm

Daytime Meinel band brightness < Nighttime Meinel band brightness

A series of images around a single orbit, frequency 0.5Hz. The party hat structure is due to the satellite nod that allows the SMR to scan the limb.

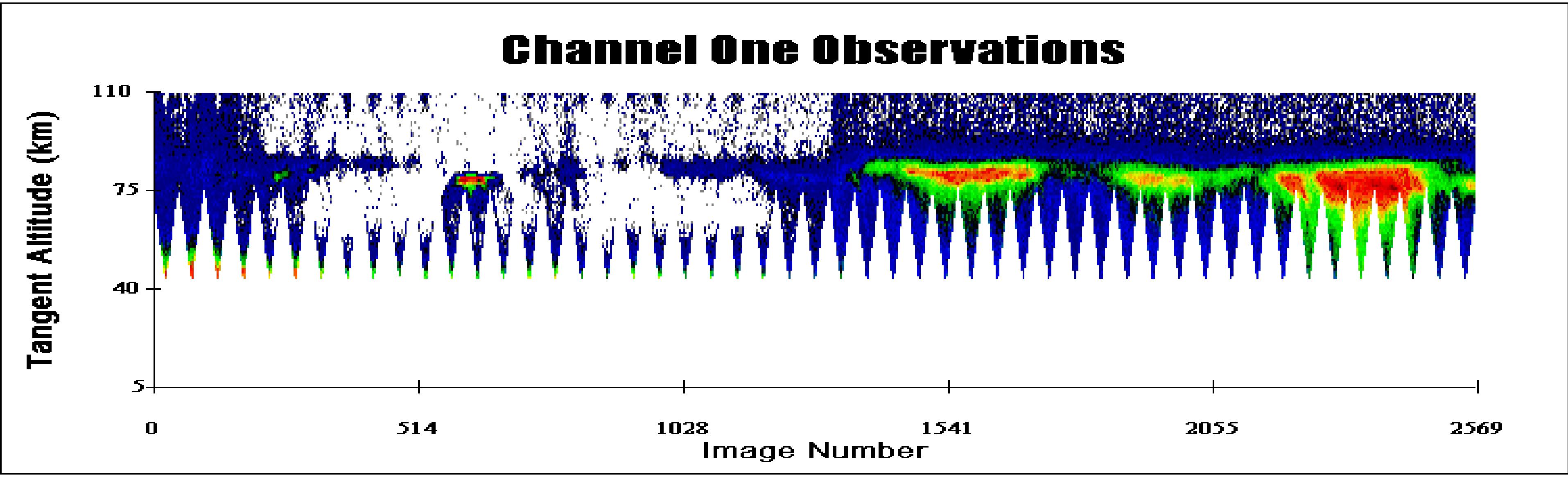

Other things seen by OSIRIS

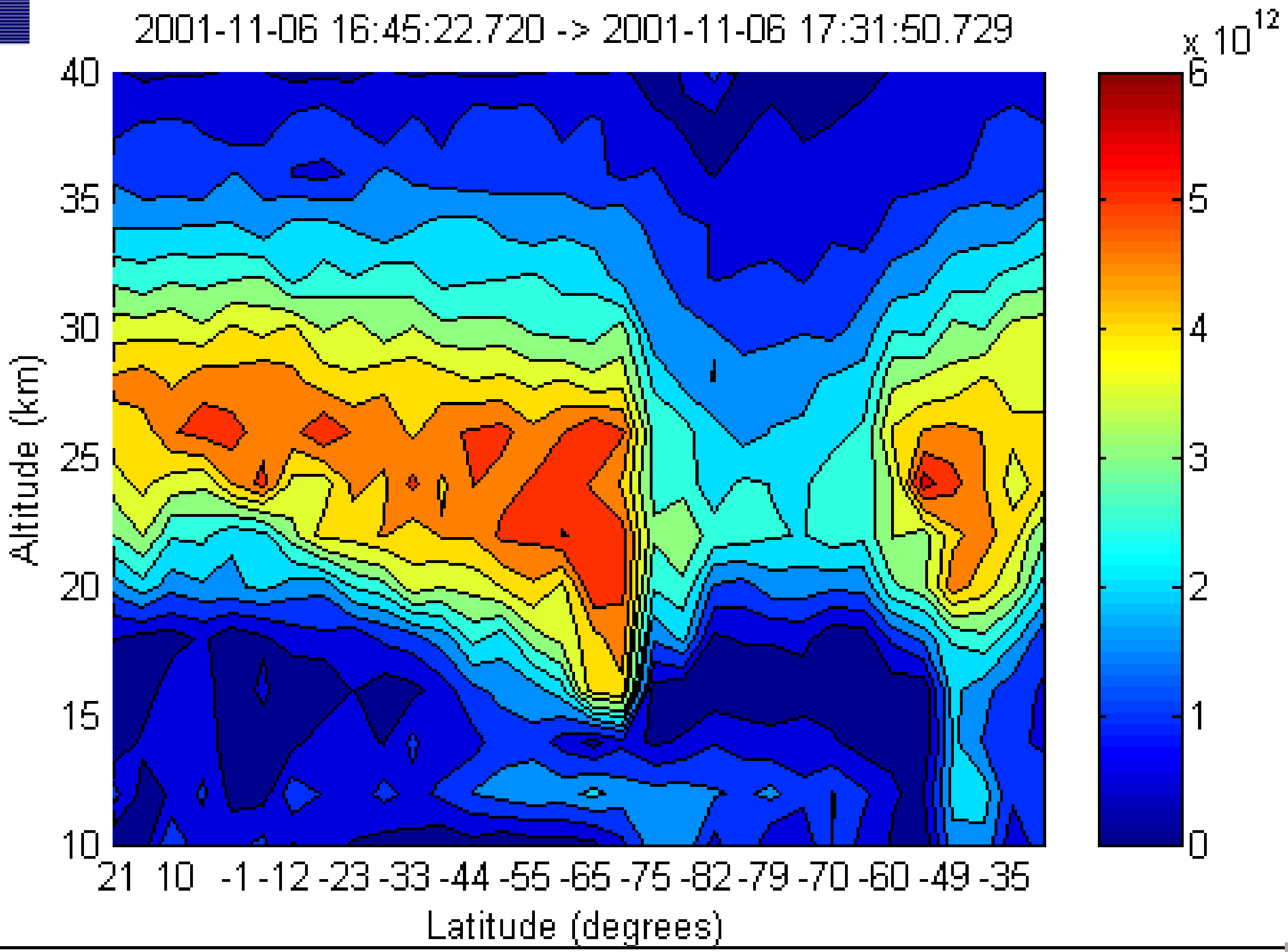
2001-11-06 16:45:22.720 -> 2001-11-06 17:31:50.729
x 10^12
Altitude (km)
40
35
30
25
20
15
10
21 10 -1 -12 -23 -33 -44 -55 -65 -75 -82 -79 -70 -60 -49 -35
Latitude (degrees)
0
1
2
3
4
5
6

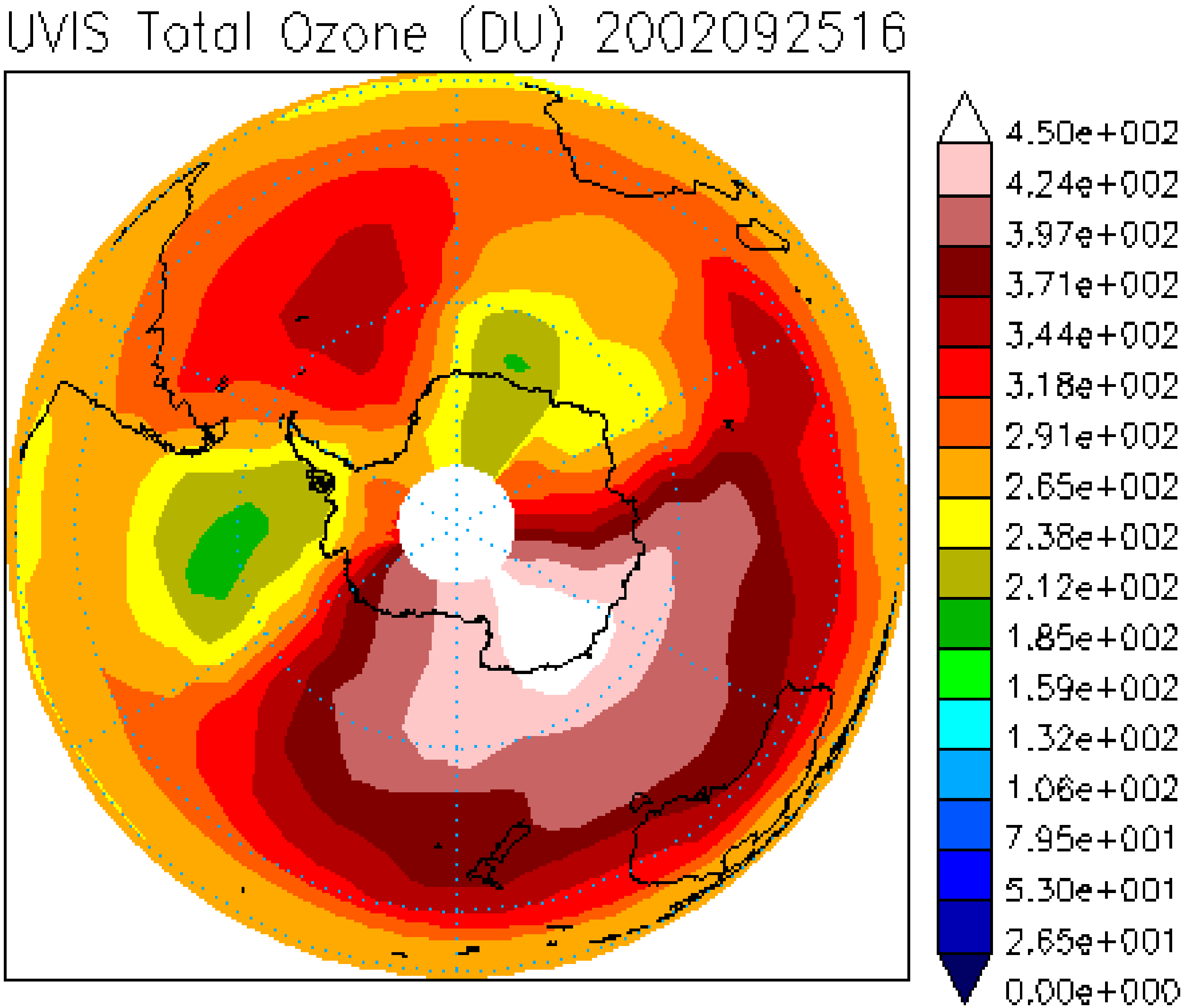
UVIS Total Ozone (DU) 2002092516
4.50e+002
4.24e+002
3.97e+002
3.71e+002
3.44e+002
3.18e+002
2.91e+002
2.65e+002
2.38e+002
2.12e+002
1.85e+002
1.59e+002
1.32e+002
1.06e+002
7.95e+001
5.30e+001
2.65e+001
0.00e+000

UVIS Ozone 10.0 km 2002092516

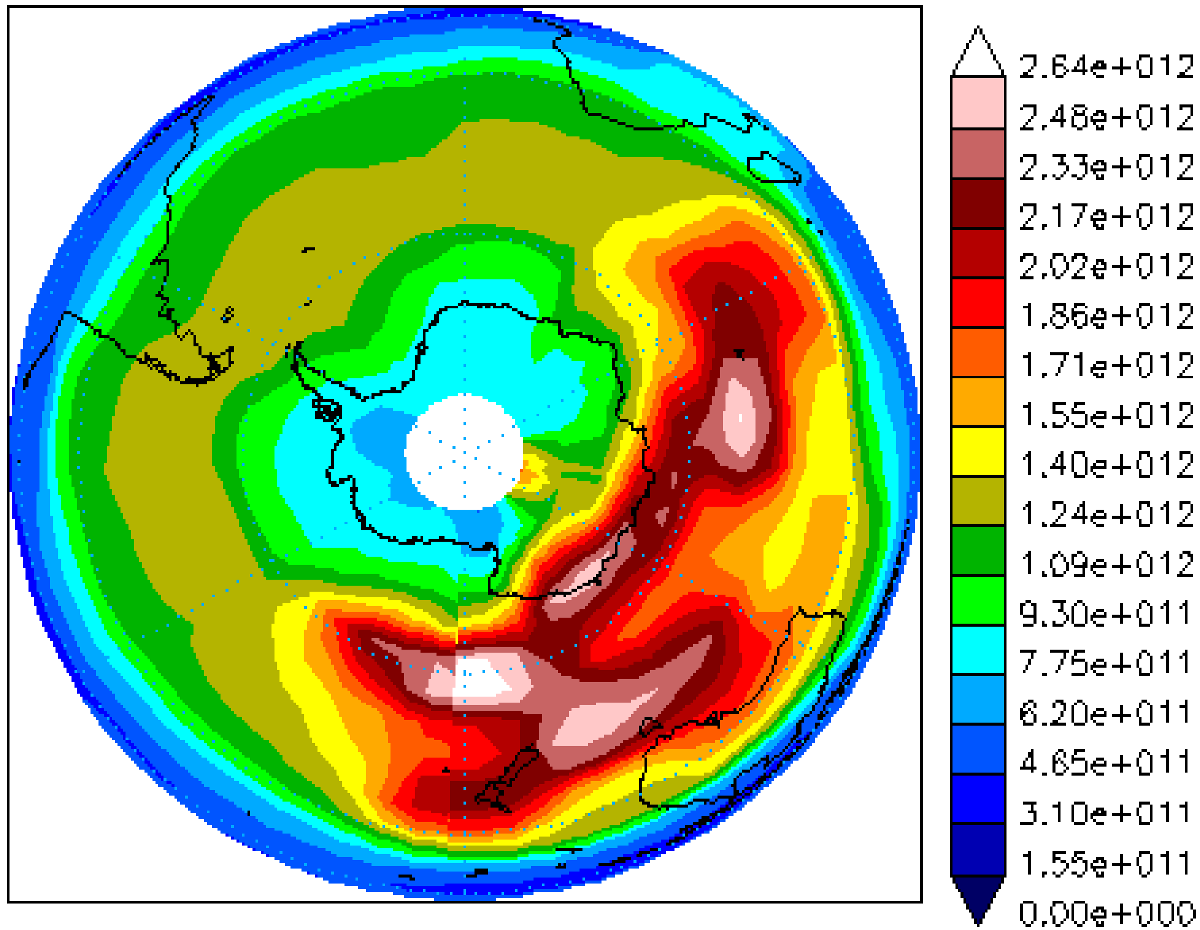

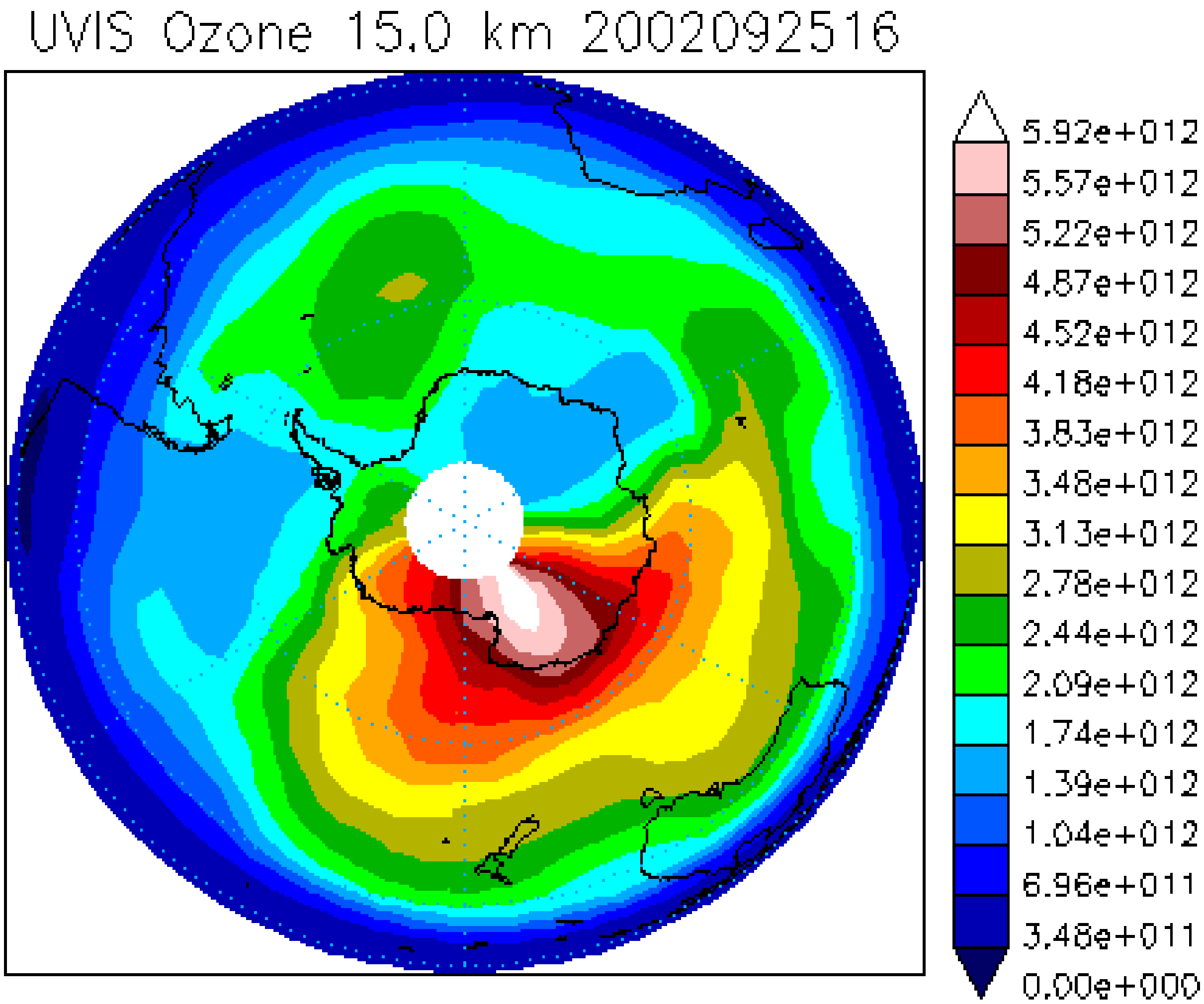
UVIS Ozone 15.0 km 2002092516
5.92e+012
5.57e+012
5.22e+012
4.87e+012
4.52e+012
4.18e+012
3.83e+012
3.48e+012
3.13e+012
2.78e+012
2.44e+012
2.09e+012
1.74e+012
1.39e+012
1.04e+012
6.96e+011
3.48e+011
0.00e+000

UVIS Ozone 20.0 km 2002092516

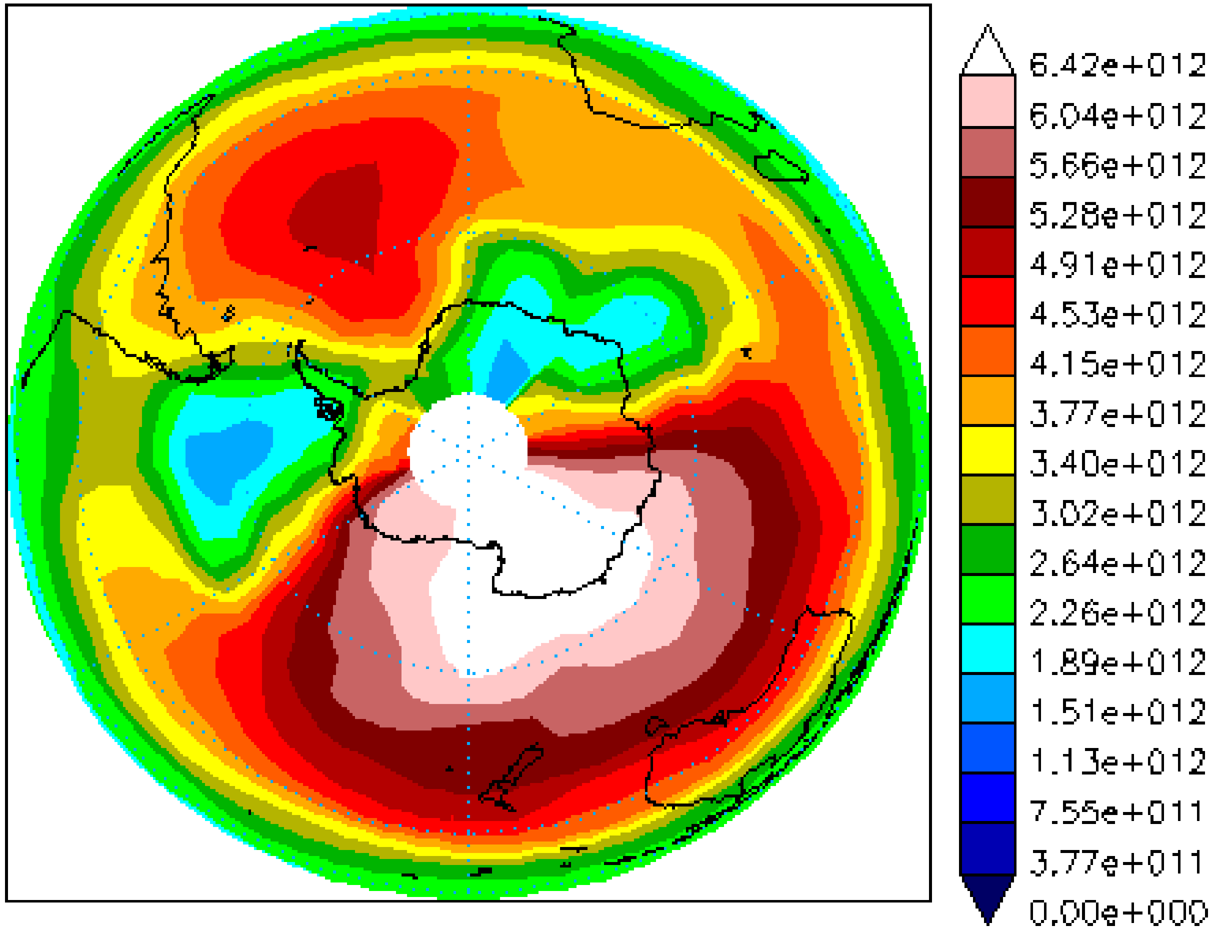

UVIS Total Ozone (DU) 2002100111

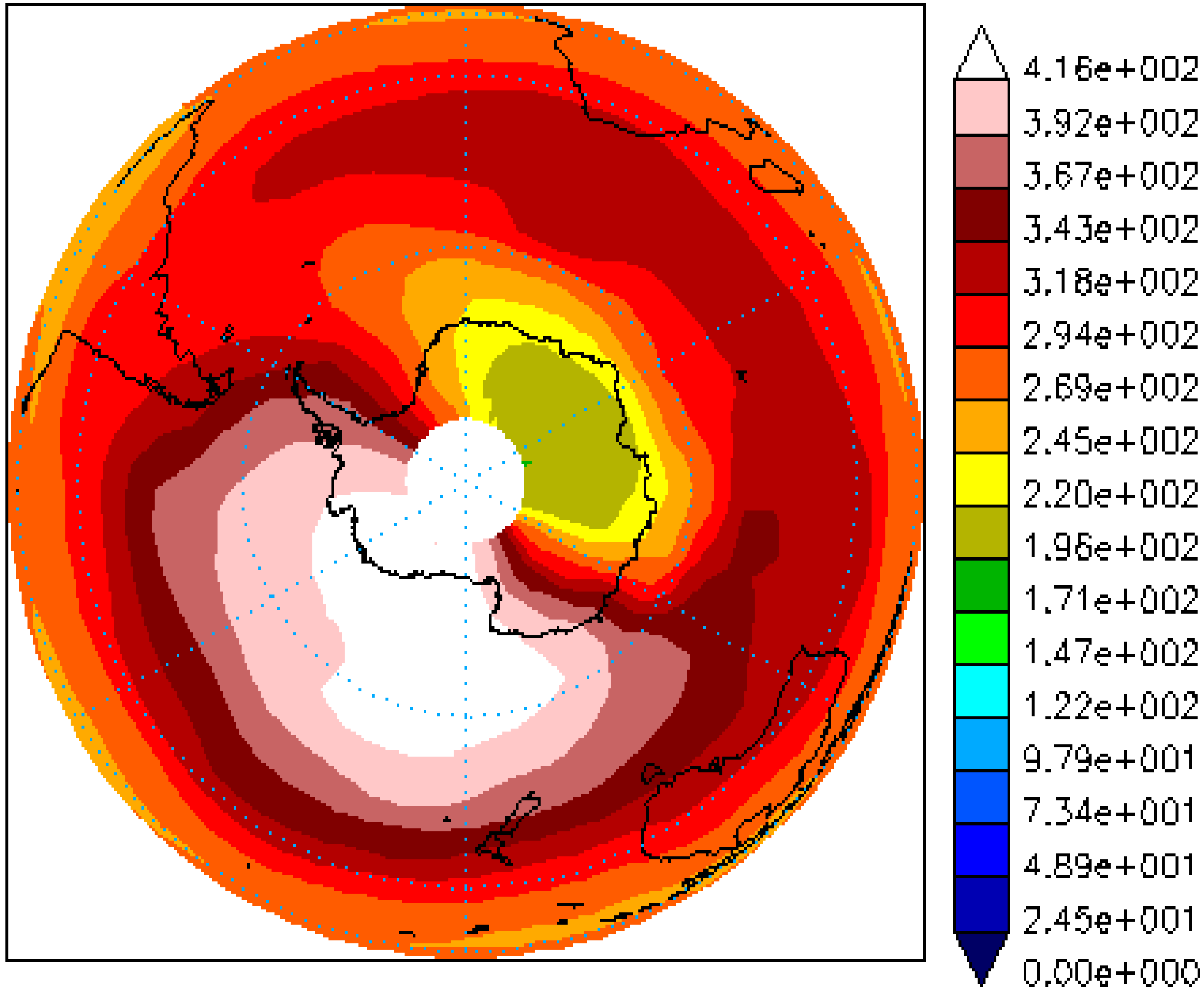

UVIS Ozone 20.0 km 2002100111

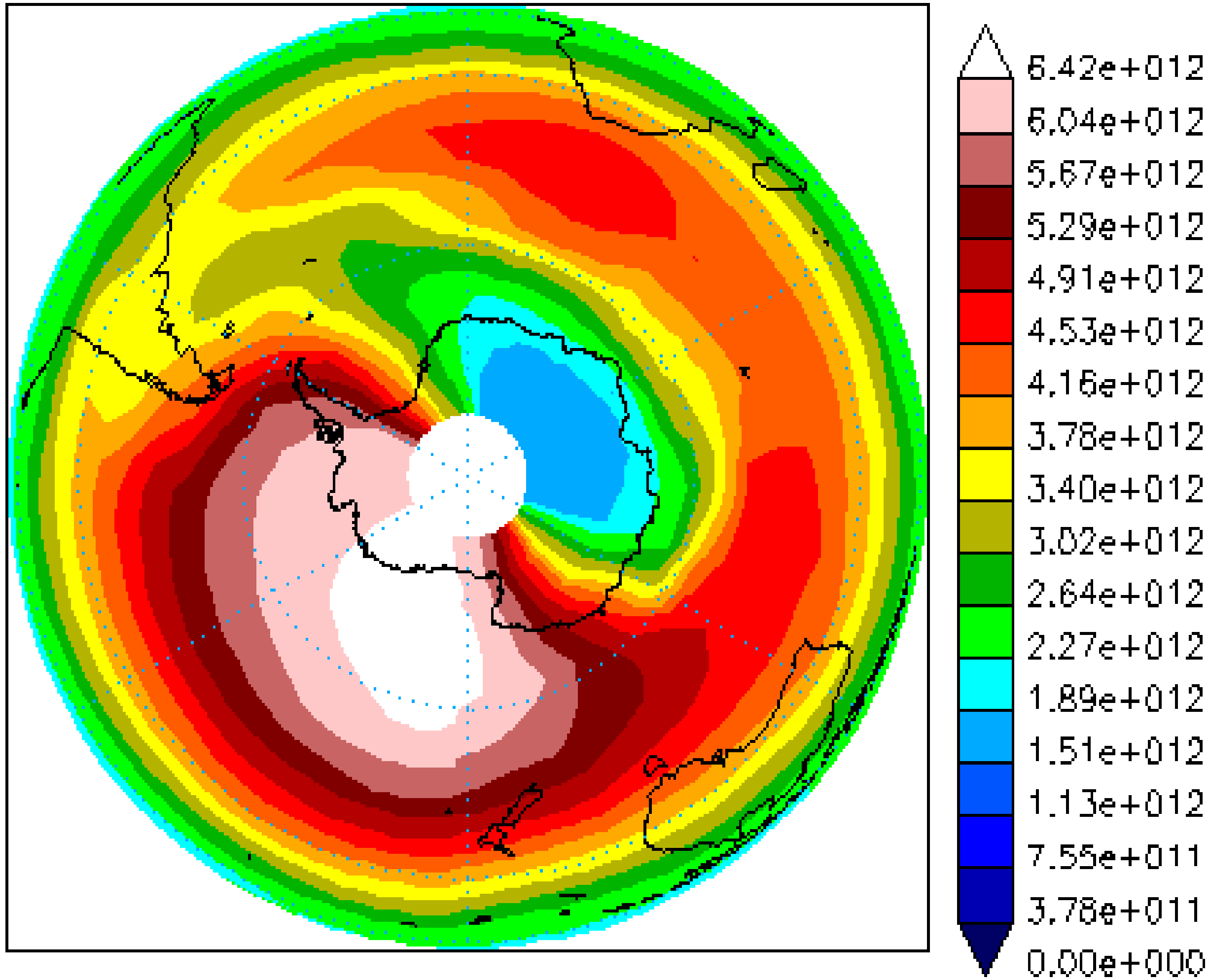

Thank you to everyone who has made the journey with OSIRIS possible.

It is an incredible feeling to be able to see things that we have only dreamed of.

References from Odin/OSIRIS Team

Page 1

N.D. Lloyd and E.J. Llewellyn, Deconvolution of Blurred Images using Photon Counting Statistics and Maximum Probability. *Can. J. Phys*., **67**, 89-94, 1989.

I.C. McDade, N.D. Lloyd and E.J. Llewellyn, A Rocket Tomography Measurement of the N2+ 3914A Emission in an Auroral Arc. *Planet. Space Sci*., **39**, 895-906, 1991.

Ian C. McDade and E.J. Llewellyn, Inversion Techniques for Recovering Two-Dimensional Distributions of Auroral Emission Rates from Tomographic Rocket Photometer Measurements. *Can. J. Phys*., **69**, 1059-1068, 1991.

Ian C. McDade and Edward J. Llewellyn, Satellite Limb Tomography: Methods for Recovering Structured Emission Rates in the Mesospheric Airglow Layer, *Can. J. Phys*., **71**, 552-563, 1993.

References Page 2

D.A. Degenstein, Atmospheric Volume Emission Tomography From A Satellite Platform, *Ph.D. Thesis*, University of Saskatchewan, 1999.

I.K. Khabibrakhmanov, D.A. Degenstein and E.J. Llewellyn, Mesospheric Ozone: Determination from orbit with the OSIRIS instrument on Odin, *Can. J. Phys*. **80**, 493-504, 2002.

D.A. Degenstein, E.J. Llewellyn and N.D. Lloyd, The potential for incorrect interpretation of atmospheric images as seen with OSIRIS, *Proceedings of the 28AM on Optical Studies of the Upper Atmosphere*, Oulu, Finland. Sodankylä Geophysical Observatory Publications **92**, 49–53, 2003

References Page 3

E.J. Llewellyn, D.A. Degenstein, N.D. Lloyd, R.L. Gattinger, S. Petelina, I.C. McDade, C. Haley, B.H. Solheim, C. von Savigny, C. Sioris, W.F.J. Evans, K. Strong, D.P. Murtagh, and J. Stegman, First Results from the OSIRIS Instrument on-board Odin, *Proceedings of the 28AM on Optical Studies of the Upper Atmosphere*, Oulu, Finland. Sodankylä Geophysical Observatory Publications **92**, 41–47, 2003.

Douglas A. Degenstein, Edward J. Llewellyn and Nicholas D. Lloyd, Volume Emission Rate Tomography From a Satellite Platform, *Applied Optics*, **41**, 1441-1450, 2003.

Douglas A. Degenstein, Edward J. Llewellyn and Nicholas D. Lloyd, Tomographic Retrieval of the Oxygen InfraRed Atmospheric Band with the OSIRIS InfraRed Imager, *Can. J. Phys.*, **82**, 501-515, 2004.

References Page 4

D.A Degenstein, N.D. Lloyd, A.E. Bourassa, R.L. Gattinger, and E.J. Llewellyn, Observations of mesospheric ozone depletion during the October 28, 2003 solar proton event by OSIRIS, *Geophys. Res. Letts.*, **32**, #3, L03S11, doi: 10.1029/2004GL021521, 2005.

D.A Degenstein, R.L. Gattinger, N.D. Lloyd, A.E. Bourassa, J.T. Wiensz and E.J. Llewellyn, Observations of a Tertiary Ozone Peak in the Mesosphere, *J. Atmos. Space Terrest. Physics*, accepted June, 2005